Forestry Canada Forêts Canada

A competition process driven growth model for red pine

S. Magnussen and D.G. Brand

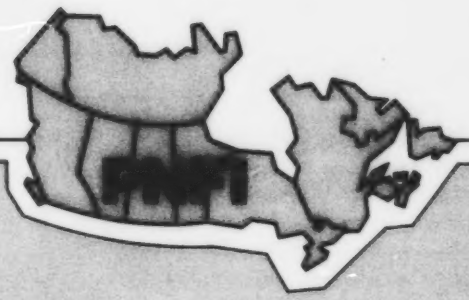

Information Report PI-X-89
Petawawa National Forestry Institute

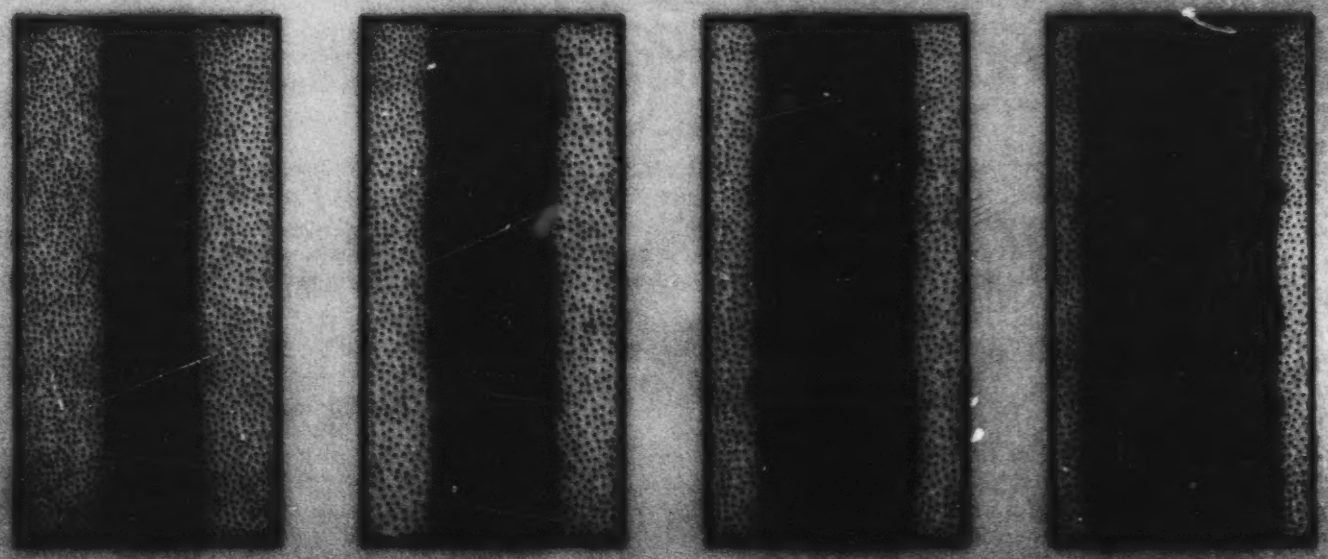

PETAWAWA NATIONAL FORESTRY INSTITUTE

In common with the rest of Forestry Canada, the Petawawa National Forestry Institute has as its objective the promotion of better management and wiser use of Canada's forest resource to the economic and social benefit of all Canadians. Objectives of program activities carried out at the Institute support this goal through discovery, development, demonstration, implementation, and transfer of innovations. Because it is a national institute, particular emphasis is placed on problems that transcend regional boundaries or that require special expertise and equipment that cannot be duplicated in Forestry Canada regional establishments. Such research is often performed in close cooperation with staff of the regional centres, provincial forest services, and the forest industry.

Research initiatives and technical services at the Institute encompass five major activities:

FOREST GENETICS AND BIOTECHNOLOGY — Integrates projects in tree genetics, soil microbiology, micropropagation, molecular genetics, meteorology, and seed research. It also includes the client services and seed bank operations of the National Tree Seed Centre, a long-standing program with extensive international affiliations.

FOREST MANAGEMENT SYSTEMS — This program integrates projects in fire, remote sensing, modelling, growth and yield, and forest pest management to provide research and development for the formulation and demonstration of forest management systems.

NATIONAL FOREST RESOURCE STATISTICS — Provides biological, technical, and socioeconomic information on Canada's forest-based resources. The program involves progressive development of databases and establishment of new databases and software in support of policy development in forestry. The Forest Inventory Program collates information on the forest resource at a national level, maintains the Canadian Forest Resources Data System, and prepares the national forest inventory.

COMMUNICATIONS — Integrates activities of the library, public awareness, information, and editing and publications projects. The Institute is visited by more than 20 000 people every year. There is a Visitor Centre for the public, self-guided tours, and an extensive education project. The national repository of all scientific and technical publications of the Forestry Canada and the principal Forestry Canada publications distribution centre are both located at PNFI.

THE RESEARCH FOREST — Besides natural stands manipulated in a variety of ways for silvicultural research, the 100 km^2 Petawawa Forest contains extensive areas of plantations dating back six decades. Research plantations are a source of growth and yield data derived from cultural experiments, and they are becoming valuable for pedigreed genetic materials for micropropagation and molecular genetics studies. The forest also offers opportunities for short- and long-term testing of forest management strategies.

A COMPETITION PROCESS DRIVEN GROWTH MODEL FOR RED PINE

S. Magnussen and D.G. Brand

Information Report PI-X-89
Petawawa National Forestry Institute
Forestry Canada
1989

90-00224/

©Minister of Supply and Services Canada 1989
Catalogue No. Fo46-11/89-1989E
ISBN 0-662-17013-X
ISSN 0706-1854
Printed in Canada

Copies of this publication may be obtained free of charge from the following address:

Forestry Canada
Publications Distribution Centre
Petawawa National Forestry Institute
Chalk River, Ontario
K0J 1J0

Telephone: 613-589-2880

A microfiche edition of this publication may be purchased from:

Micromedia Ltd.
Place du Portage
165, Hôtel-de-Ville
Hull, Québec
J8X 3X2

Cette publication est également disponible en français sous le titre
Modèle de croissance du pin rouge fondé sur le processus de compétition.

Contents

v Abstract/Résumé

1 Introduction

1 Model description

3 The database

4 Data summary

4 Stem volume
4 Stem numbers

5 Regression models of stem volume, volume increment, and relative growth rate

5 Simulation model

5 Maximum relative growth rate
7 Plot and age specific estimation of parameters a and b
7 Modelling a and b as a function of the plot relative density index (RDI)
11 Simulation of stochastic disturbances

12 Mortality

13 Statistical validation of model output

14 Simulation results and validation

14 Comparisons of individual plot model predictions and observed values
14 Comparisons of general model predictions and observed values

26 Discussion and conclusions

36 References

Tables

6 1. Average (observed) stem volume (dm^3 over bark) in plots of different ages and spacings. Standard deviations are enclosed in brackets
6 2. Mean absolute error in per cent of predicted stem volume (RMAE), and the coefficient of determination (RSQ) in the nonlinear regressions of single tree stem volume as a function of age (see equation [2])
8 3. Regression estimates of *a* and *b* obtained from the model in equation [1]. Standard errors of estimates are provided in brackets
11 4. Estimates of c_1-c_4 in equations [7] and [8]
13 5. Average correlation among random numbers (Z) used to generate random deviations of a and b
t = age subscript
13 6. Average probability (P_{mort}) that a tree will die in any given year
22 7. Comparisons of individual plot model predictions with 'observed' values of mean volume, maximum volume, relative growth rate, and mean annual increment
33 8. Comparisons of general model predictions with observed values of mean volume, maximum volume, relative growth rate, and mean annual increment

Figures

2 1. The general relationship between relative growth rate and relative tree size (tree size divided by the median size). RGR_{max} is a potential upper limit of growth. Curves t_1 to t_6 illustrates the change in relative growth rate over time ($t_6 > t_5 > ... > t_1$) as competition intensifies.

2 2. Growth vigour index (*d*) as a function of *b* and relative tree size (*s*). Model: $d = a \bullet (1-e^{b \bullet s})$ with $a = 0.50$.

4 3. Flowchart of model.

5 4. Stems per hectare from ages 10 to 35 years from planting in plots used for validation of the general prediction model.

7 5. Boundary line (RGR_{max}) and observed relative growth rates (maxima of 0.018 m^3-wide size classes) in the six plots used to derive the general model (see equation [5]).

10 6. Regression models of the relationship between competition parameter *a* (see equations [1] and [7] for details) and the relative density index (*RDI*). Parameter estimates are given in Table 4.

10 7. Regression models of the relationship between competition parameter *b* (see equations [1] and [8] for details) and the relative density index (*RDI*). Parameter estimates are given in Table 4.

15 8. Individual plot model predictions (full line) and observed values (dashed line) of mean, maximum, and minimum stem volume. Vertical bars indicate the 68% confidence interval (2x standard deviation of predictions) for the predictions.

16 9. Individual plot model predictions (full line) and observed values (dashed line) of mean **RGR** (curves descending from left to right) and **MAI** (curves ascending from left to right). Vertical bars indicate the 68% confidence interval (2x standard deviation of predictions) for the predictions.

17 10. Individual plot model predictions (full line) and observed values (dashed line) of stem volume standard deviation (σ), skewness (γ_1), and kurtosis (γ_2). Vertical bars indicate the 68% confidence interval (2x standard deviation of predictions) for the predictions.

19 11. Individual plot model predictions (white bars) and observed values (black bars) of stem size (class width 0.018 m^3) frequencies. Vertical bars indicate the 68% confidence interval (2x standard deviation of predictions) for the predictions.

24 12. General model predictions (full line) and observed values (dash line) of mean, maximum, and minimum stem volume. Vertical bars indicate the 68% confidence interval (2x standard deviation of predictions) for the predictions.

25 13. General model predictions (full line) and observed values (dash line) of mean **RGR** (curves descending from left to right) and **MAI** (curves ascending from left to right). Vertical bars indicate the 68% confidence interval (2x standard deviation of predictions) for the predictions.

27 14. General model predictions (full line) and observed values (dash line) of stem volume standard deviations (σ), skewness (γ_1), and kurtosis (γ_2). Vertical bars indicate the 68% confidence interval (2x standard deviation of predictions) for the predictions.

29 15. General model predictions (white bars) and observed values (black bars) of stem size (class width 0.018 m^3) frequencies. Vertical bars indicate the 68% confidence interval (2x standard deviation of predictions) for the predictions.

Abstract

A simulation model, predicting individual tree growth and mortality, is developed using data from a red pine spacing trial. Changes in relative growth rates as related to changes in tree size, the size of the individual tree relative to the median population size, and the overall stand density are central elements of the model. The model parameters are biologically interpretable as measures of the process of competition. Data from six spacings were used to develop the model whereas a different data set from eight spacings served to validate the model. Inclusion of random but correlated error components provided the basis for stochastic simulations. Based on individual stem volume and stand area at age 10 as input, the model was used to predict trends in tree volume distributions until age 35. A detailed graphical representation of model output (summary statistics of stem volume distributions) is presented and compared with observed data. Prediction errors of most results were as a rule below 25%; smaller errors were associated with shorter prediction periods. It is concluded that the model realistically generates the temporal dynamics of volume distributions in even-aged red pine plantations. Failure to predict stand development beyond a square spacing of 3.0 m, and poor predictions for the 1.2 m, spacing limits model application to initial spacings between 1.5 m and 3.0 m. The limited requirement for input data makes the model an attractive tool for growth and yield simulation.

Résumé

Un modèle de simulation de la croissance et de la mortalité des individus a été construit à l'aide des expériences sur l'espacement des plantations de pins rouges. Les changements des taux de croissance relatifs se rapportant à la taille des arbres, à la taille des individus par rapport à la taille moyenne de la population et à la densité du peuplement en général sont les principaux éléments du modèle. Du point de vue biologique, les paramètres du modèle permettent de mesurer le processus de compétition. Les données provenant de six essais d'espacement ont servi à créer le modèle qui a été validé par les résultats des huit autres essais d'espacement. Les simulations stochastiques s'appuient sur l'inclusion d'erreurs aléatoires, mais corrélatives. À partir du volume individuel des tiges et de la superficie d'un peuplement âgé de 10 ans, le modèle permet de prévoir la tendance dans la distribution du cubage des arbres jusqu'à l'âge de 35 ans. Les résultats obtenus à l'aide du modèle (résumé statistique de la distribution du cubage) sont présentés au moyen d'un graphique détaillé et ils sont comparés aux données d'observations. En général, la marge d'erreur des prévisions était inférieure à 25 % et alle était plus faible pour des périodes de prévision plus courtes. Les auteurs arrivent à la conclusion que le modèle reproduit de façon réaliste la dynamique temporelle de la distribution du cubage dans une plantation équienne de pins rouges. En raison de l'échec des prévisions de la croissance d'un peuplement pour un espacement en quinconce de plus de 3 m et du manque de précision pour un espacement de 1,2 m, l'application du modèle est restreinte à des espacements initiaux variant entre 1,5 et 3 m. Puisqu'un petit nombre de données d'entrée suffit à créer le modèle, celui-ci se révèle un outil intéressant pour simuler la croissance et la possibilité.

A COMPETITION PROCESS DRIVEN GROWTH MODEL FOR RED PINE

Introduction

Models of forest growth have long been used by forest managers to support decision making (Avery and Burkhart 1983). Reliable predictions, of mean tree attributes and stems per hectare at different ages, were the main purpose of most management models in the past (Borders and Bailey 1986, Clutter et al. 1983, Ek 1974). Because the future distribution of stem sizes is essential to the solution of a broad array of problems associated with forest management, a new class of models, including those predicting the size distribution of stands, were developed. This new class of models predicts the parameters of a known distribution function from whole stand variables. This, in turn, allows a breakdown of total yield into specified size-classes (Bailey 1980, Bailey and Dell 1973, Hyink and Moser 1983, Magnussen 1986). Apart from compatibility between growth and yield (Clutter 1963) and various other mathematical constraints, such models do not attempt to reflect the dynamics of stand growth, only its outcome (Clutter et al. 1983, Hann and Ritchie 1988).

Although both the process and importance of inter-tree competition on stand development are well known (Ford 1975, Hamilton 1969, Perry 1985, Westoby 1982) progress towards a growth model that is consistent with the body of current theory has been slow (Holdaway 1984, Hyink and Moser 1983). Recent attempts to incorporate the "-3/2 power rule of self thinning" into existing model structures do little to elucidate the underlying process of competition; they only describe an idealized outcome (Hardwick 1987, Sterba 1975, Yoda et al. 1963, Zeide 1987). Several published theoretical studies and simulation models still await empirical evaluation (Aikman and Watkinson 1980, Ford and Diggle 1981, Hara 1984). Spatial models with competition indices assigned to each tree as a growth modifier have extensive input requirements that have limited their practical use (Alemdag 1978, Martin and Ek 1984, Wykoff et al. 1982).

The intent here is to present a framework for modeling tree growth consistent with our theory of the competition process in an even-aged plantation of forest trees. A red pine (*Pinus resinosa* Ait.) spacing trial served to validate our approach. Brand and Magnussen (1988) described the competition process in this and other spacing trials as being asymmetric and two-sided in the later stages of more intense density-stress. The proposed model reflects these findings and modifies the theoretical model of one-sided competition proposed by Aikman and Watkinson (1980). Inclusion of stochastic (random) disturbances of growth enabled repeated simulations to be run and computation of standard errors for the predicted outcome.

Model description

Tree growth is the net balance between anabolic gains (constructive metabolism) and catabolic losses (destructive metabolism) (Tait 1988). The former is generally proportional to available photosynthetically active radiation (PAR) while the latter is proportional to plant weight (Harper 1977).

After canopy closure trees begin to compete for light through crown encroachments among neighbouring trees. Gradually less vigourous trees will receive less and less PAR and their growth rate will decline or eventually cease due to reduced constructive metabolism. The process of competition tends to exaggerate initial differences in size through the development of a hierarchy of resource exploitation. Competition can be described in terms of symmetry and one- or two-sidedness. Symmetry implies that resources are shared in relation to size (Weiner and Thomas 1986). Two-sided competition infers that all population members are affected to some degree. With one-sided competition larger plants affect the growth of smaller neighbours only. In studying the competition process, it is important to use measures of tree vigour or efficiency, rather than size. Otherwise the size of the tree is a greater determinant of growth than the influence of competition and determining the specific process of competition is made difficult. A sensitive measure of a tree's response to its competitive environment is the relative growth rate (Ford 1975, Perry 1985).

As stand density increases the relationship between relative growth rate (RGR) and tree size undergoes progressive change. In open grown young stands the highest relative growth rates are commonly found in smaller sized trees, whereas the opposite is true in older stands (Perry 1985, Weiner and Thomas 1986). Figure 1 displays a general pattern of progressive changes in the relationship between tree size and growth rate (Perry 1985). Curve t1 is for a young, open-grown stand within which there is a minimum of competition while t6 represents the curve for an older stand within which there is intense competition.

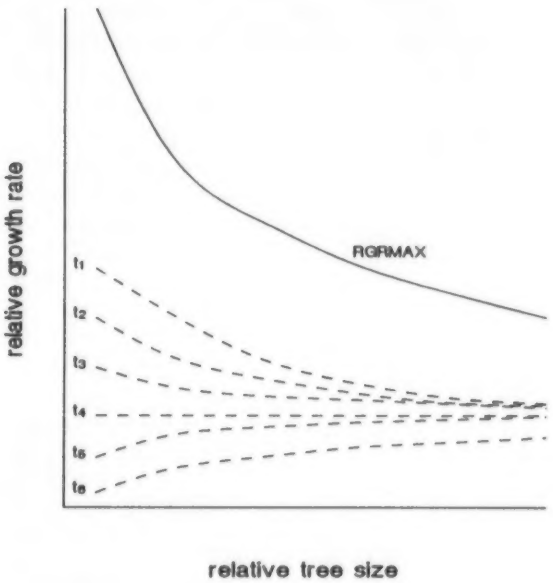

Figure 1. The general relationship between relative growth rate and relative tree size (tree size divided by the median size). RGR_{max} is a potential upper limit of growth. Curves t_1 to t_6 illustrates the change in relative growth rate over time ($t_6 > t_5 > ... > t_1$) as competition intensifies.

Figure 1 shows that the negative effects of competition on growth appear first in the smallest trees, but spread to increasingly larger trees as competition intensifies. In the later and most intensive phases of competition all members of the population have reduced growth due to the overall density of the stand. Brand and Magnussen (1988) have described this process in greater detail. We concluded that competition in red pine is asymmetric (resource sharing is not strictly proportional to size) and that competition progresses from a one-sided (only small trees suffers reductions in growth) to a two-sided (bigger trees are also effected by competition) process as stand density increases.

To model the relationship between relative growth rate and tree size can therefore by a very complex task (Aikman and Watkinson 1980). However, the complexity can be reduced considerably by introducing the concepts of an upper limit to the relative growth rate (RGR_{max}) that defines site quality and a growth modifier or index of growth vigour $d = RGR/RGR_{max}$ that defines the competition, microsite, and genetic effects. When d is plotted against the size of a tree relative to the median size of the population the dynamic changes over time can be described by a single family of exponential functions. Figure 2 illustrates a transformation of the relative growth rates in Figure 1 to relative vigour indices. The curves can all be described by the function

$$[1] \quad d = RGR/RGR_{max} = a(1-e^{-b \cdot s})$$

where s is the relative tree size (s = size/median size), a and b are parameters of downward one-sided competition (b) and of two-sided competition (a). The a-parameter affects all trees regardless of size, whereas the magnitude of b indicates the extent of competition effects in individual size classes (see Figure 2). High b-values

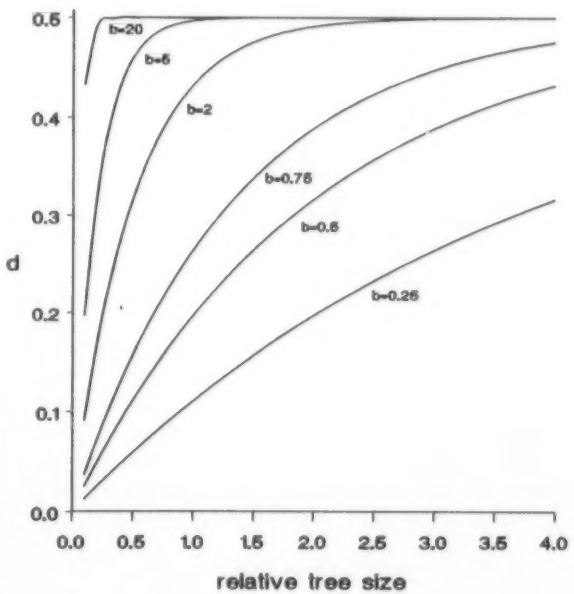

Figure 2. Growth vigour index (*d*) as a function of *b* and relative tree size (*s*). Model: $d = a \cdot (1-e^{b \cdot s})$ with $a = 0.50$.

(b>20) indicate that virtually no trees are affected by competition, and low b-values (b<0.5) show that all stand members suffer from growth reductions due to competition. Although the parameters can be associated with one-sidedness and two-sidedness of the competition process, it doesn't necessarily mean that this separation can be upheld when fitting data to this model. Correlations among a and b will tend to obscure the distinction.

The model projects stem volume growth of individual red pine (*Pinus resinosa* Ait.) trees growing in an even-aged plantation. Initial spacing of the plantation is assumed to be uniform (square). Growth is estimated from a site specific relationship between tree size (stem volume), maximum relative growth rate (RGR_{max}), and the growth modifier d ($0 \leq d \leq 1$). The relationship between tree size and maximum relative growth rate simply recognizes that, as trees increase in size, the net balance between anabolic and catabolic processes decreases. Thus larger trees have lower potential growth rates than small ones.

A tree's vigour index (d) is influenced by (i) a tree's status in the size hierarchy of the stand, (ii) the overall density (volume) of the plantation, and (iii) apparently random (positive or negative) deviations from the norm in individual tree conditions (including genetics), microsites and local competition. Tree status was measured as size relative to the median size of the population (the median was preferable to the mean as a measure of central tendency due to its distribution-free properties). Population (or plantation) densities were measured by a relative density index (RDI), which is the ratio between the actual mean tree volume and the theoretical maximum (Smith and Hann 1984) for a given number of live stems per hectare.

Tests of the model in equation [1] revealed a poor fit at the lower extreme of tree size distribution. Growth of small trees were consistently overestimated. By subtracting half the minimum tree size from all tree volumes before dividing them by the median, we obtained a much improved model fit for these very small trees (e.g. $s = (vol - vol_{min}/2)/median)$).

Mortality can be either density induced (i.e. concentrated in smaller trees) or random (porcupine damage, lightning, windthrow, insects and diseases) (Belli and Ek 1988, Buchman 1985). In the version of the growth model presented, a simple life-table (age of death known for each tree) was used to account for mortality. An integrated modelling approach to mortality is presented in a later section. Every tree that died in the sample plots were eliminated after the growing season in which they died. Details about mortality recordings are given by Brand and Magnussen (1988).

A summary of the sequence of individual steps in the growth model is shown in Figure 3. The stochastic elements of growth were introduced via random but correlated "errors" in the variables of the model. Growth predictions would, therefore, vary from one run of the model to the next. A stable prediction of mean volume* was obtained after 25 growth simulations for a particular plantation. All model predictions are based on this number of simulations.

The database

A red pine spacing trial, established in 1953 on abandoned agricultural lands now belonging to Atomic Energy of Canada Ltd. (Chalk River, Ontario), and consisting of windblown sands overlaying glacial-fluvial outwash, provided the data used for model development and verification.

The experiment included plantations of 1.2, 1.5, 1.8, 2.1, 2.4, and 3.0 m square spacing. In addition, an area of 2.1 metre spacing was systematically thinned to 4.3 metre spacing at age 5** and an area of 3.0 metre spacing was systematically thinned to 6.0 m spacing at age 8**. At the point of re-spacing, minimal inter-tree competition was occurring and trees had live branches to ground level. Dead trees were refilled after the first growing season. The plantations were measured in 1962 and then every five years to 1987. Measurements included stem diameter at 1.37 m above ground level for all trees, and heights for a representative sample from each diameter class. Remaining heights were estimated from height-diameter regressions. To increase the accuracy of stem volume calculations, a series of sample trees were measured for stem diameter at 1.52 m intervals up the tree. Stem volume (outside bark) was then calculated from taper equations developed for each plot (Stiell and Berry 1977). A summary of the stem volume data is presented in Table 1.

*The moving average changed by less than 1% between successive simulations.
**From planting.

Figure 3. Flowchart of model.

Data summary

Stem volume

Average stem volume increased markedly with available initial tree spacing (Table 1). At age 10 the average stem volume in the widest spacing (3.0 m) was 3.5 times as large as the average volume in the 1.2 m plots. This relationship was more or less maintained until age 25. Beyond age 25, the widely spaced (≥3.0 m) plots enjoyed a continued rapid increase in mean stem volume whereas growth in denser plots was visibly slowed. Accordingly, the ratio of mean volumes of widely spaced plots to that of denser plots kept rising.

Stem numbers

Self thinning was evident in both the 1.2 m and the 1.5 m spacing (Figure 4). In the former, mortality increased dramatically from around age 20, while in the latter mortality commenced at age 25. Density-induced mortality became apparent in the 1.8 m spacing after age 30 (Figure 4). Plots with wider spacings showed no signs of self-thinning during the measurement period.

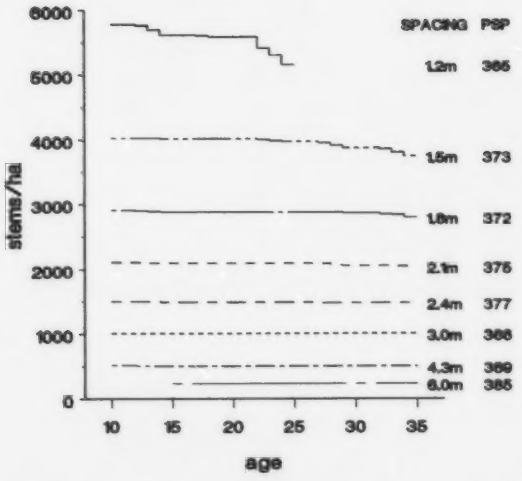

Figure 4. Stems per hectare from ages 10 to 35 years from planting in plots used for validation of the general prediction model.

Regression models of stem volume, volume increment, and relative growth rate

Stem volume (V) at any age (t) between the first and last measurement of a given tree was predicted from age using a three parameter Richards function (Hunt 1982) fitted to the observed data. (Regression estimates of a parameter x, say, is denoted by x to distinguish it from the error free value x.)

$$[2]\quad V_t = V_\infty/(1+e^{(h-k\bullet t)})$$

where V_t is estimated stem volume, V_∞ is the estimated hypothetical asymptotic stem volume for $t\rightarrow\infty$ (Shifley and Brand 1984), k is a growth rate determining constant, and h determines the inflection point. The ratio h/k equals the age where predicted volume is half its asymptotic value. Fit statistics of the least squares solutions are presented in Table 2. Predicted volumes at age 15 explained with one exception over 93% of the variation in the observed data (see RSQ in Table 2). Predictions of age 20 and older stem volumes accounted for 98% - 99.9% of the variance encountered (exception: 6.0 m spacing). A poor fit was obtained with the 10 years' results and with data from the 6.0 m spacing. The relative mean absolute prediction error amounted in most spacings to no more than 1-3% for trees aged 25 years and older. Age 15 and age 20 results were, as a rule, predicted with relative mean absolute error of approximately 10%. A combination of poor fit (RSQ~0) and low volume figures made the relative prediction errors at age 10 very high.

Estimation of stem volume growth (VI_t) at time t was derived for a single tree via the first derivative of equation [2] with respect to time.

$$[3]\quad VI_t = V_\infty\bullet k\bullet e^{(h-k\bullet t)}/(1+e^{(h-k\bullet t)})^2$$

From [3] and [2] the relative stem volume growth rate (RGR_t) at time t of an individual tree was found to be

$$[4]\quad RGR_t = VI_t/V_t = k\bullet e^{(h-k\bullet t)}/(1+e^{h-k\bullet t})$$

All above estimates were used as 'observed' values in the derivation and validation of the simulation model. The satisfactory fit of the Richards function to the actual observations justifies this approach.

Simulation Model

Maximum relative growth rate

The hypothesized relationship between tree size and maximum relative growth rate (RGR_{max}) was defined as the upper limit of 'observed' values of RGR versus size. Relative growth rates (see equation [4]) were computed for all trees beginning at the age of the first measurement, and further for every third year until the last measurement or mortality occurred. Individual size class (width 5 dm^3) maxima of relative growth rate are plotted against the corresponding mid-class stem volume in Figure 5. The boundary line displayed served as the estimator of maximum relative growth rate. It can be expressed mathematically as

$$[5]\quad RGR_{max} = \begin{cases} 0.94\text{-}5.739\bullet V \text{ for } V \le 0.01\ m^3 \\ e^{(1/(-1.2833+0.5763\bullet \ln(V)))} \text{ for } V > 0.01 m^3 \end{cases}$$

It is evident that sections of this boundary line have been determined from data in different spac-

Table 1. Average (observed) stem volume (dm^3 over bark) in plots of different ages and spacings. Standard deviations are enclosed in brackets.

Spacing, m (PSP)	Plot size, m^2	Age*											
		10		15		20		25		30		35	
1.2 (364)	1010	6	(3)	17	(8)	39	(22)	63	(36)	-		-	
1.2 (365)	1010	5	(3)	17	(8)	38	(20)	60	(32)	-		-	
1.5 (373)	1010	11	(5)	24	(9)	46	(17)	75	(31)	106	(47)	130	(61)
1.5 (374)	1010	11	(5)	24	(9)	47	(18)	77	(33)	109	(50)	137	(64)
1.8 (371)	1010	13	(5)	29	(11)	59	(21)	97	(36)	131	(53)	156	(66)
1.8 (372)	1010	13	(5)	30	(10)	60	(20)	98	(35)	134	(51)	161	(63)
2.1 (368)	1010	17	(6)	40	(13)	83	(26)	142	(46)	196	(67)	232	(81)
2.1 (375)	1010	15	(6)	38	(14)	82	(30)	143	(53)	203	(73)	239	(88)
2.4 (376)	1010	16	(6)	39	(14)	88	(29)	161	(50)	232	(72)	279	(88)
2.4 (377)	1010	17	(7)	42	(15)	92	(30)	167	(53)	243	(76)	295	(95)
3.0 (366)	1010	20	(8)	50	(17)	113	(33)	211	(56)	309	(81)	374	(100)
3.0 (378)	1010	21	(8)	53	(17)	121	(33)	229	(59)	339	(91)	415	(115)
4.3 (369)	2020			42	(17)	105	(37)	225	(66)	373	(76)	484	(115)
6.0 (385)	4050			72	(20)	166	(37)	337	(60)	563	(92)	761	(132)

*from planting. Age from seed is obtained by adding four years to table entries.

Table 2. Mean absolute error in per cent of predicted stem volume (RMAE*), and the coefficient of determination (RSQ**) in the nonlinear regressions of single tree stem volume as a function of age (see equation [2]).

Spacing (PSP) m	Age											
	10		15		20		25		30		35	
	RMAE	RSQ	RMAE	RSQ	RMAE	RSQ	RMAE	RSQ	RMAE	RSQ	RMAE	RSQ
1.2 (364)	0.248	0.811	0.062	0.987.	0.002	0.997	0.006	0.998	-	-	-	-
1.2 (365)	0.196	0.930	0.049	0.991	0.015	0.997	0.005	0.998	-	-	-	-
1.5 (373)	0.846	0.283	0.038	0.984	0.084	0.987	0.019	0.998	0.046	0.996	0.020	0.999
1.5 (374)	0.907	0.129	0.040	0.980	0.085	0.987	0.020	0.997	0.049	0.996	0.022	0.999
1.8 (371)	0.945	0.327	0.035	0.987	0.079	0.990	0.016	0.998	0.038	0.996	0.039	0.999
1.8 (372)	0.999	0.362	0.036	0.986	0.077	0.991	0.016	0.997	0.039	0.996	0.019	0.999
2.1 (368)	1.047	0.480	0.040	0.979	0.082	0.990	0.016	0.998	0.028	0.998	0.015	0.999
2.1 (375)	1.171	0.404	0.044	0.982	0.078	0.993	0.015	0.999	0.002	0.998	0.013	0.999
2.4 (376)	1.517	0.019	0.099	0.977	0.082	0.990	0.012	0.997	0.033	0.998	0.015	0.999
2.4 (377)	1.577	0.103	0.097	0.963	0.087	0.991	0.013	0.997	0.033	0.997	0.015	0.999
3.0 (366)	1.674	0.000	0.133	0.962	0.080	0.987	0.018	0.996	0.039	0.995	0.016	0.999
3.0 (378)	2.000	0.000	0.170	0.960	0.086	0.991	0.023	0.995	0.042	0.996	0.017	0.999
4.3 (369)	1.603	0.000	0.362	0.934	0.072	0.981	0.032	0.995	0.029	0.997	0.009	0.999
6.0 (385)	-	-	0.442	0.741	0.574	0.738	0.466	0.774	0.382	0.843	0.266	0.869

*RMAE = $(\sum_i |obs_i - pred_i|)/\sum_i obs_i$

**RSQ = $(1-\sigma^2_{residual})/\sigma^2_{observed}$ = coefficient of determination.

ings. As volume increases the influence of denser plots diminish and the more widely spaced plots increasingly serve to define RGR_{max}.

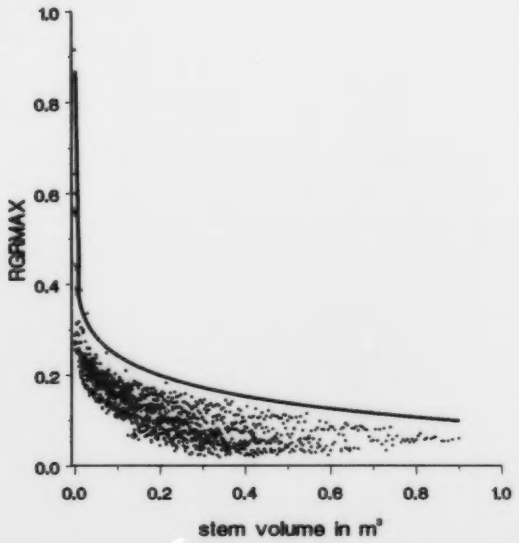

Figure 5. Boundary line (RGR_{max}) and observed relative growth rates (maxima of 0.018 m^3-wide size classes) in the six plots used to derive the general model (see equation [5]).

Plot and age specific estimation of parameters a and b.

Predictions of the growth vigour index (*d*) from relative tree size (see equation [1]) appeared feasible in stands with a distinct size hierarchy and established inter-tree competition. In such stands the model explained 46%-88% of the observed variance in *d* and allowed predictions of *d* with a standard error of 0.02-0.04. In stands with a weak or no inter-tree competition, d was nearly constant for any relative tree size and the model approached (through high *b*-values) a straight line with zero slope throughout most of its range. Prediction errors of *d* during this early growth phase were, as a rule, two to three times larger than during periods with strong competition.

Nonlinear regression estimates of *a* and *b* are listed in Table 3. The two estimates are in most cases highly and negatively correlated (Table 3). Estimates of a varied from 0.48 to 0.70 at age 13, when competition in most plots was negligible. This range illustrates how growth vigour (realized growth) can vary from one plot to another in the absence of competition. Compared to the magnitude of the standard errors of a, it is concluded that the realized growth potential (d) varied significantly among plots. a tended to decline rapidly with age as competition (b<2) intensified. Estimates of *b* were in the range 0.55-100. An exponential decline was observed in all plots between ages 19 and 34. Estimates of *b* at age 13 were lower than estimates at age 19 in three plots (374, 376, 378). However, in these cases the age 13 values of b were sufficiently high (b>7) to preclude any competition effects in the plots. This reversal of the age trend in *b* is, therefore, not significant in practice, and it can be safely ignored in the modelling process that follows.

Modelling a and b as a function of the plot relative density index RDI

Both *a* and *b* change in a regular manner over time. However, these changes are difficult to interpret without a measure of the intensity of competition in the plots. A relationship between plot density and the above parameters was therefore deemed desirable. Drew and Flewelling (1979) introduced the relative density index (*RDI*) as the ratio between the observed mean stand volume (V) and a hypothesized maximum (V_{max}) mean volume for a given number of trees per hectare (N). The maximum mean tree volume was obtained by plotting values of ln(V) against the logarithm of the live number of trees per hectare in the plot. The apparent upper limit of these plotted points defined the boundary line or V_{max}. Using the same data as in this study, Smith and Hann (1984) found the following expression for the relative density index (subscripts refer to age)

$$[6]\quad RDI_t = V_t/V_{max} = V_t/(e^{10.077-1.47\bullet\ln(N)})$$

where N is the number of trees per hectare. Using this density index, the following functional relationships between *a* and *b* and *RDI* were postulated:

$$[7]\quad a = c_1\bullet(1-e^{c_2/RDI})$$

$$[8]\quad b = c_3\bullet e^{c_3\bullet RDI}$$

Estimates of the four parameters c_1-c_4 were obtained through non-linear least-squares applied to the results presented in Table 3.

Table 3. **Regression estimates of *a* and *b* obtained from the model in equation [1]. Standard errors of estimates are provided in brackets.**

Spacing (PSP)	Age	a (s.e.)	b (s.e.)	R(a,b)*	S_{regr}**	RSQ(d,s)***
1.2 m (364)	13	0.702 (0.013)	1.54 (0.08)	-0.90	0.11	0.60
	16	0.697 (0.013)	1.47 (0.07)	-0.91	0.10	0.71
	19	0.669 (0.017)	1.01 (0.05)	-0.95	0.08	0.77
	22	0.533 (0.017)	0.81 (0.05)	-0.96	0.06	0.76
	25	0.371 (0.019)	0.61 (0.05)	-0.97	0.04	0.72
1.5 m (374)	13	0.464 (0.012)	7.07 (2.04)	-0.45	0.14	0.00
	16	0.462 (0.009)	5.89 (3.36)	-0.29	0.11	0.10
	19	0.470 (0.010)	2.26 (0.12)	-0.87	0.02	0.75
	22	0.516 (0.016)	1.09 (0.07)	-0.94	0.05	0.82
	25	0.575 (0.027)	0.68 (0.05)	-0.97	0.04	0.88
	28	0.539 (0.027)	0.54 (0.06)	-0.97	0.04	0.87
	31	0.529 (0.036)	0.36 (0.06)	-0.98	0.04	0.85
	34	0.427 (0.018)	0.32 (0.09)	-0.96	0.03	0.77
1.8 m (371)	13	0.497 (0.002)	14.12 (1.76)	-0.15	0.04	0.20
	16	0.495 (0.002)	6.26 (0.38)	-0.49	0.03	0.36
	19	0.487 (0.003)	3.11 (0.13)	-0.71	0.03	0.68
	22	0.468 (0.004)	1.99 (0.09)	-0.82	0.04	0.70
	25	0.445 (0.007)	1.28 (0.07)	-0.92	0.04	0.79
	28	0.414 (0.013)	0.84 (0.07)	-0.97	0.04	0.79
	31	0.387 (0.021)	0.539 (0.07)	-0.99	0.03	0.78
	34	0.340 (0.022)	0.37 (0.07)	-0.99	0.02	0.75

*R (a,b) = asymptotic correlation of estimates

**S_{regr} = standard error of regression

***RSQ(d,s) = coefficient of determination between d and s, given the model in equation[1]

Table 3 (cont'd)

Spacing (PSP)	Age	a (s.e.)	b (s.e.)	R(a,b)	S_{regr}	RSQ(d,s)
2.1 m (368)	13	0.558 (0.005)	4.55 (0.33)	-0.62	0.05	0.67
	16	0.564 (0.003)	4.21 (0.26)	-0.63	0.03	0.77
	19	.550 (0.004)	3.53 (0.25)	-0.67	0.05	0.47
	22	0.516 (0.007)	2.60 (0.19)	-0.80	0.05	0.42
	25	0.464 (0.010)	1.85 (0.16)	-0.91	0.05	0.49
	28	0.404 (0.017)	1.27 (0.14)	-0.96	0.05	0.52
	31	0.353 (0.026)	0.82 (0.13)	-0.98	0.04	0.46
	34	0.272 (0.019)	0.62 (0.14)	-0.98	0.03	0.49
2.4 m (376)	13	0.585 (0.003)	6.46 (1.28)	-0.23	0.05	0.05
	16	0.596 (0.004)	10.37 (3.82)	-0.20	0.06	0.00
	19	0.592 (0.005)	7.02 (1.58)	-0.23	0.06	0.00
	22	0.553 (0.005)	5.08 (1.12)	-0.29	0.06	0.00
	25	0.479 (0.006)	3.78 (0.66)	-0.52	0.06	0.17
	28	0.384 (0.008)	2.80 (0.41)	-0.76	0.06	0.25
	31	0.291 (0.010)	2.01 (0.31)	-0.88	0.05	0.29
	34	0.214 (0.012)	1.41 (0.27)	-0.94	0.04	0.33
3.0	13	0.627 (0.004)	16.18 (3.05)	-0.16	0.04	0.72
	16	0.655 (0.009)	18.38 (11.84)	1.00	0.08	0.20
	19	0.657 (0.008)	100.* -	-	0.08	0.00
	22	0.621 (0.012)	21.10 (0.65)	-0.72	0.08	0.00
	25	0.599 (0.016)	2.54 (0.35)	-0.86	0.08	0.04
	28	0.551 (0.024)	1.50 (0.24)	-0.94	0.07	0.39
	31	0.520 (0.039)	0.85 (0.20)	-0.98	0.06	0.52
	34	0.549 (0.073)	0.441 (0.19)	-0.99	0.04	0.53

*Upper limit reached.

A graphical display of the regression solutions to [7] and [8] are displayed in Figures 6 and 7; the numerical results are given in Table 4. The prediction model proposed for *a* provided reasonably accurate results for three plots (371, 368, and 376), and a rather poor accuracy for two plots (364, 378) at medium to high relative densities (RDI > 0.4). For one plot (374), the c_2 parameter was so high that the prediction model led to a virtually constant *a* value throughout most of the range of *RDI*. It is quite clear that each plot (spacing) follows an unique *a* trajectory for increasing values of *RDI* and that statistically significant differences must exist among plots (no formal testing was done). However, it was not possible to establish any consistent relationship between spacing and the model parameters c_1 and c_2 (Pearson's correlation coefficients were less than 0.19).

Apparently, random rank changes in the a-values of plots between high (RDI > 0.8) and low (RDI < 0.2) relative densities (Spearman rank correlations were below 0.1) add further complications. Two plots (371 and 374) caused this low correlation; the remaining four plots showed no rank changes. One common feature among a majority of plots is the relative constancy of a until RDI reaches a value of approximately 0.2. Beyond this density a declines at an average rate of 0.03 for every 0.1 increase in RDI. Simple averages for c_1 and c_2 served as parameters in the general prediction model. This average model predicts a 10% decline in a when RDI goes from 0.01 to 0.3. At RDI = 0.7 this decline amounts to 30%. In effect, as stand density increases, competition becomes more two-sided.

Parameters c_3 and c_4 were derived from a reduced data set. Owing to irregular trends in b at low RDI-values (see Table 3) and the limited significance of *b*-values above 5 it was decided to restrict the regression analyses to RDI values above 0.3. Estimates of c_3 and c_4 are listed in Table 4 and a graphical display of the individual plot models is presented in Figure 7. In spite of generally high coefficients of determination (RSQ), *b* was estimated with a substantial error. The model for plot 378 (3 m spacing) predicts much lower *b*-values for any RDI-value than any other. At the other extreme was plot 376 (spacing 2.4 m).

This contrasting behaviour by the two most widely spaced plots supports the contention of no

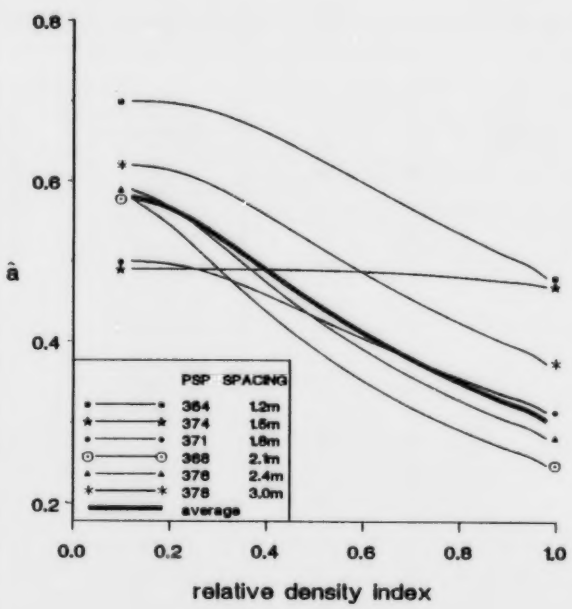

Figure 6. Regression models of the relationship between competition parameter *a* (see equations [1] and [7] for details) and the relative density index (*RDI*). Parameter estimates are given in Table 4.

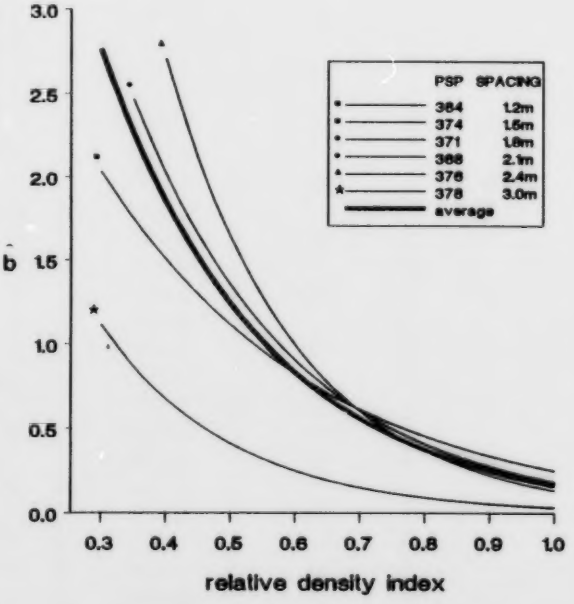

Figure 7. Regression models of the relationship between competition parameter *b* (see equations [1] and [8] for details) and the relative density index (*RDI*). Parameter estimates are given in Table 4.

spacing effects on the level of *b* for a given *RDI*. A b value of 2 or higher is found in most plots with RDI below 0.3, which indicates that only trees smaller than the median tree are affected by one-sided competition (see Figure 2). Virtually all the trees had their growth depressed by competition once b was less than 0.5 (see Figure 2). This seems to occur in most plots when *RDI* exceeds 0.7. Simple averages of c_3 and c_4 were used for general predictions of *b* from RDI.

Simulation of stochastic disturbances

The sequential nature of the model is shown in Figure 3; at the beginning of each sequence the model parameters are 'updated' according to established deterministic relationships and new growth is predicted. Moreover, to generate realistic predictions, the probabilistic nature of the model parameters must be taken into consideration (Harrison and Stevens 1976). This was done by generating stochastic variation in the parameters *a*, *b*, and *d*. It follows from the sequential nature of the predictions that these sources of variation become integrated in future predictions; the model is driven by past predictions (Harrison and Stevens 1976). Disturbances (errors) were limited to the parameters *a*, *b*, and *d*. The remaining parameters RGR_{max} and V_{max} are associated with unknown bias and their potential influence is built into the site specificity of our regression estimates of *a*, *b*, and *d*. Observed correlations among estimates and residuals were used to simulate realistic disturbances at all levels.

Stochastic elements were added in the growth simulation at steps 4 and 5 of the model (Figure 3). The parameters *a* and *b* in step 4 are subject to three kinds of errors:

ε_{a1}, ε_{b1} = error of estimate for a given age in a given plot

ε_{a2}, ε_{b2} = error in predictions of *a* and *b* via *RDI* (see Table 4).

ε_{a3}, ε_{b3} = whole plot error due to plot specific deviations from the average model.

In step 5 the average growth vigour index *d* for an individual tree with a relative size *s* was determined from the parameters *a* and *b*. Individual *d*-values, in turn, were obtained by ad-

Table 4. Estimates of c_1-c_4 in equations [7] and [8]

Spacing (PSP)	c_1	c_2	$S_{regr.}$***	RSQ****	c_3**	c_4**	$S_{regr.}$	RSQ
1.2 (364)	0.70	-0.86	0.08	0.48	5.0	-3.0	0.24	0.98
1.5 (374)	0.49	-3.17*	0.05	0.00	5.0	-3.0	0.19	0.93
1.8 (371)	0.50	-0.99	0.01	0.95	10.0	-4.0	0.10	0.99
2.1 (368)	0.58	-0.56	0.03	0.88	10.0	-4.0	0.12	0.97
2.4 (376)	0.59	-0.35	0.05	0.84	20.0	-5.0	0.22	0.99
3.0 (378)	0.62	-0.92	0.03	0.26	5.0	-5.0	0.32	0.32
Avg.	0.58	-0.74	-	-	9.17	-4.0		

*not included in the average (outlier)
**excluding observations for which RDI <0.3
***S_{regr} = standard error of regression
****RSQ = coefficient of determination

ding a random error (ε_d) to the regression predictions.

All random deviations were generated from appropriate estimates of error-variances (σ^2_ε) and normally distributed "pseudo random" numbers (Z) with mean zero and a variance of one (Fishman and Moore 1982). Correlations (temporal and otherwise) among errors were generated through modifications or restrictions on Z (Ripley 1987).

Estimates of the error variances $\sigma^2_{\varepsilon a1}$ and $\sigma^2_{\varepsilon b1}$ associated with ε_{a1} and ε_{b1}, respectively, were obtained from the following least squares solutions

$$[9]\quad \sigma^2_{\varepsilon a1} = (0.0794 \bullet a - 0.0965 \bullet a^2)^2$$

$$[10]\quad \sigma^2_{\varepsilon b1} = (0.1319 \bullet b + 0.0004 \bullet b^2)^2$$

Both equations were obtained by fitting the standard errors in Table (3) to a quadratic function of the estimated parameters (a and b, respectively). Expression of $\sigma^2_{\varepsilon a2}$ and $\sigma^2_{\varepsilon b2}$ was approximated by linear regressions of observed variances of estimates on the estimates themselves, i.e.

$$[11]\quad \sigma^2_{\varepsilon a2} \approx (0.09 \bullet a)^2$$

$$[12]\quad \sigma^2_{\varepsilon b2} \approx (0.10 \bullet b)^2$$

Finally, approximations of $\sigma^2_{\varepsilon a3}$ and $\sigma^2_{\varepsilon b3}$ were obtained by a Taylor series expansion of [7] and [8] around the mean value of c (Gellert et al. 1975)

$$[13]\quad \sigma^2_{\varepsilon a3} \approx (1-e^{c_2/RDI_t})^2 \bullet \sigma^2_{c_1} + (c_1/RDI_t \bullet e^{c_2/RDI_t})^2 \bullet \sigma^2_{c_2} - 2/RDI_t \bullet e^{c_2/RDI_t} \bullet \sigma_{c_1,c_2}$$

$$[14]\quad \sigma^2_{\varepsilon b3} \approx (\varepsilon^{c_4} \bullet RDI_t^{c_3} \bullet \sigma^2_{c_3} + (RDI_t \bullet c_3)^2 \bullet (e^{c_4} \bullet RDI_t)^2 \bullet \sigma^2_{c_4} + 2 \bullet RDI_t \bullet e^{c_4} \bullet RDI_t \bullet \sigma_{c_3,c_4}$$

where c_i and $\sigma^2_{c_i}$ denote the mean and variance, respectively, of individual plot estimates of c_i (i=1,2,3,4) (see Table 4 for details). $\sigma_{c_i c_j}$ stands for the sample covariance of plot estimates c_i and c_j. Using the sample means c_1=.58, c_2=-0.74, c_3=9.17, c_4=-4 and the following among-plot variances and covariances of the c-parameters $\sigma^2_{c_1}=0.08^2$, $\sigma^2_{c_2}=0.27^2$, $\sigma^2_{c_3}=3.67^2$, $\sigma^2_{c_4}=0.89^2$, $\sigma_{c_1c_2}=0.0054$, and $\sigma_{c_3c_4}=-0.72$ solutions to [13] and [14] for any *RDI* value can be obtained.

Adding $\sigma^2_{\varepsilon a2}$ to $\sigma^2_{\varepsilon a1}$ yields the within-plot error variance of a. The same for b was found as $\sigma^2_{\varepsilon b2} + \sigma^2_{\varepsilon b1}$.

The final random component added to a in year t was then computed as

$$[15]\quad \varepsilon_{a,t} = Z_{a,t} \bullet \sqrt{\sigma^2_{\varepsilon a1} + \sigma^2_{\varepsilon a2}} + Z_{a,plot} \bullet \sigma_{\varepsilon a3}$$

where

$Z_{a,t}$ is the random disturbance used for a at time t; $Z_{a,plot}$ is a plot (simulation) specific random number. A new $Z_{a,plot}$ value was generated for each initialization of the growth process (step 1 in Figure 3). $\varepsilon_{b,t}$ was obtained in a manner similar to [15]. Correlation analyses of regression residuals indicated that the correlations displayed in Table 5 provides a mechanism to simulate residuals with desired properties. Algorithms for generating random numbers, subject to the restrictions in Table 5, are given by Ripley (1987), for example.

Random deviations of d for individual trees at age t were computed as

$$[16]\quad \varepsilon_{d,t} = Z_{d,t} \bullet \sigma_{d,t}$$

where $\sigma_{d,t}$ is the standard error of the predicted average value of d for trees of relative size s. $\sigma_{d,t}$ could be expressed as a function of the relative density index (*RDI*) at time t.

$$[17]\quad \sigma_{d,t} = 0.062 - 0.024 \bullet RDI_t$$

Residual analysis indicated a strong correlation among $Z_{d,t}$ values over time. A one year lag correlation of 0.8 was deemed appropriate for all ages (i.e. $r(\varepsilon_{d,t}, \varepsilon_{d,t-1}) = 0.8$). Correlations among residuals of different trees were assumed to be zero.

Mortality

All dead trees in the database were assigned an age of death. Ages were determined by choosing an integer at random within the time period during which death was known to have occurred. When a tree reached its age of death during the

Table 5. **Average correlation among random numbers (Z) used to generate random deviations of a and b.**
t = age subscript.

	$Z_{a,t-1}$	$Z_{a,t}$	$Z_{b,t-1}$	$Z_{b,t}$	$Z_{a,plot}$	$Z_{b,plot}$
$Z_{a,t-1}$	1.0	0.7	-0.9	-0.3	0	0
$Z_{a,t}$		1.0	-0.3	-0.9	0	0
$Z_{b,t-1}$			1.0	0.5	0	0
$Z_{b,t}$				1.0	0	0
$Z_{a,plot}$					1.0	0
$Z_{b,plot}$						1.0

growth simulations it was automatically deleted from the stand being modeled.

Although no attempt was made to model or simulate tree mortality it was noted that mortality was indeed closely related to the growth vigour index (*d*). The probability that a tree would die in any given year (P_{mort}) increased with decreasing d-values. Table 6 gives the empirical values obtained from analysis of the entire database. Including these mortality probabilities in the model would allow an integrated modelling approach to stochastic simulation of the mortality process.

Table 6. **Average probability (P_{mort}) that a tree will die in any given year**

Growth vigour index $d \times 10^3$	$P_{mort} \times 10^2$
0-5	4.2
6-15	1.4
16-25	1.9
26-35	0.9
36-45	0.7
46-55	0.3
56-65	0.3
66-75	0.2
76-85	0.1
≥86	0.0

Statistical validation of model output

The repeated stochastic simulation of stem-volume growth enabled the calculation of a standard deviation of model predictions. This standard deviation is considered an unbiased estimate of the standard error of predictions. The sampling errors associated with the observed plot values were ignored in most cases (exceptions: standard deviations of observed values and maximum stem volume). Ordinary t-tests were performed to make inference about the significance of the difference between model predictions and 'observed' values. 'Observed' is here understood as summary statistical results derived directly from the individual tree growth equations described in an earlier section (page 5).

t-tests were performed under the following assumptions: (i) variance of a variance is equal to the squared variance divided by its degrees of freedom, (ii) the standard error of an extreme value (maximum) is equal to one-half the sample standard deviation, (iii) the standard deviation of skewness is equal to $\sqrt{6/n}$ where n = sample size, and (iv) the standard deviation of kurtosis is equal to $\sqrt{24/n}$ (Snedecor and Cochran 1971).

Statistical inferences about the observed and predicted size-class distribution of stem volumes were based on three tests: 1) a Kolmogoroff-Smirnov test of the maximum difference in the cumulative density distributions, 2) a runs-test of sign-sequences in the deviations, and 3) a multivariate Hotellings T-test. The 5% risk level of accepting the 'no-difference' hypothesis when it is

wrong was chosen as the cut-off point for assessing statistical significance.

Simulation results and validation

Simulation results are illustrated in Figures 8 to 15 and in Tables 7 and 8. They are all based on 25 simulations of individual tree growth and stand development from an initial set of stem volumes at the age of the first measurement (see Figure 3).

Comparisons of individual plot model predictions and observed values

Predictions of growth using plot specific parameters (c_1,.., c_4) are displayed in Figures 8 to 11 and a quantitative comparison with observed values is given in Table 7.

Mean stem volume was predicted within 10% of the observed values in four plots representing the 1.2 m to 2.1 m spacing. Larger relative deviations were encountered in the 2.4 and 3.0 m spacings. With a prediction standard error of approximately 6%, only mean stem volume deviations in excess of 10% were statistically significant (5% risk level or lower). Negative deviations prevailed in all plots throughout the prediction period. An initial underestimation of growth rates during the first five years caused this bias in stem volumes and hence of relative growth rates which are directly related to tree size (see model derivation).

Maximum stem volume was prone to a larger error (average 8%), which is essentially the error in predictions for a single tree. In five plots predictions deviated less than 16% from the observed maxima; in the sixth plot (PSP364) the model overestimated the maximum value by more than 25%.

Relative growth rates (*RGR*) were predicted for a period of up to 10 years within 11% of the observed values. Substantially larger prediction errors was encountered towards the end of the time period. However, these large relative errors are based on numerically low RGR values. They signify that the biological age (size) of the trees no longer match the chronological age. Considering the sharp decline in RGR over age, such large relative errors must be expected from even minor deviations in stem volume. The sensitivity of RGR to tree size and plot density is seen in a considerable prediction error of *RGR* (average 18%).

Mean annual increment (MAI) was predicted within 15% of the observed values in five of the six plots, and there was generally no tendency towards an increase in prediction errors over time. The predicted *MAI* for the sixth plot (378) reflected a failure to describe trends in mean tree volume.

Standard deviations of simulated stem-volume were generally slightly underestimated by the models, but all observed values were well within twice the standard error of prediction. However, the hypothesis $\sigma_{pred} = \sigma_{obs}$ tested with Bartlett's U statistic of variance homogeneity could only be accepted (at the 5% risk level) within the first 10 years of predictions in five plots. Predictions in the 1.2 m spaced plots failed the test after just five years. No significance was detected in plots 374 and 378.

Skewness of the stem volume frequency distribution was significantly positive in the 1.2 - 1.8 m plots. Predicted skewness differed significantly from the observed in those plots. In the remaining plots the agreement between model output and observed values were good.

Kurtosis of stem size distributions stayed significantly below the expected value 3.0 of a normal distribution (i.e. the distributions were flat topped). Kurtosis was significantly underestimated in plots 364 and 374 from age 18 and beyond. These statistics, however, are very sensitive and even slight changes in the overall distribution can have a serious impact on both kurtosis and skewness.

A graphical display of the predicted and observed stem volume size-class distribution is provided in Figure 11. Only two of the predicted distributions differed significantly at the 5% risk level from the observed results (plot 378 after 20 years of predictions and in plot 376 after 25 years of predictions. Tests: Kolmogoroff-Smirnov and Runs-test).

Comparisons of general model predictions and observed values

The preceding section compares the results of a single prediction mode' for all spacings (parameters (c_1,.., c_4) have been pooled across spacings). Comparisons are made with data not used for model derivation. Time trends in predicted mean and maximum stem volume

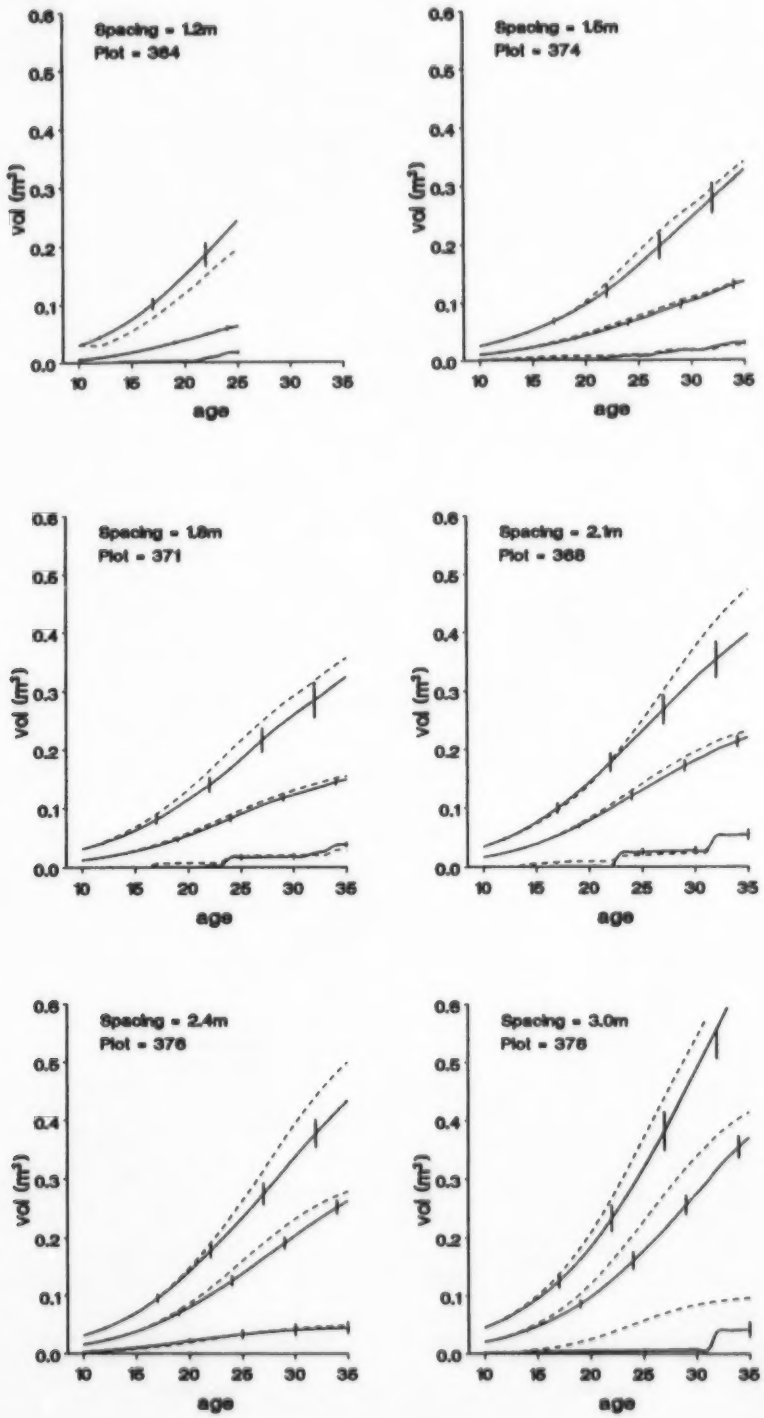

Figure 8. Individual plot model predictions (full line) and observed values (dashed line) of mean, maximum, and minimum stem volume. Vertical bars indicate the 68% confidence interval (2x standard deviation of predictions) for the predictions.

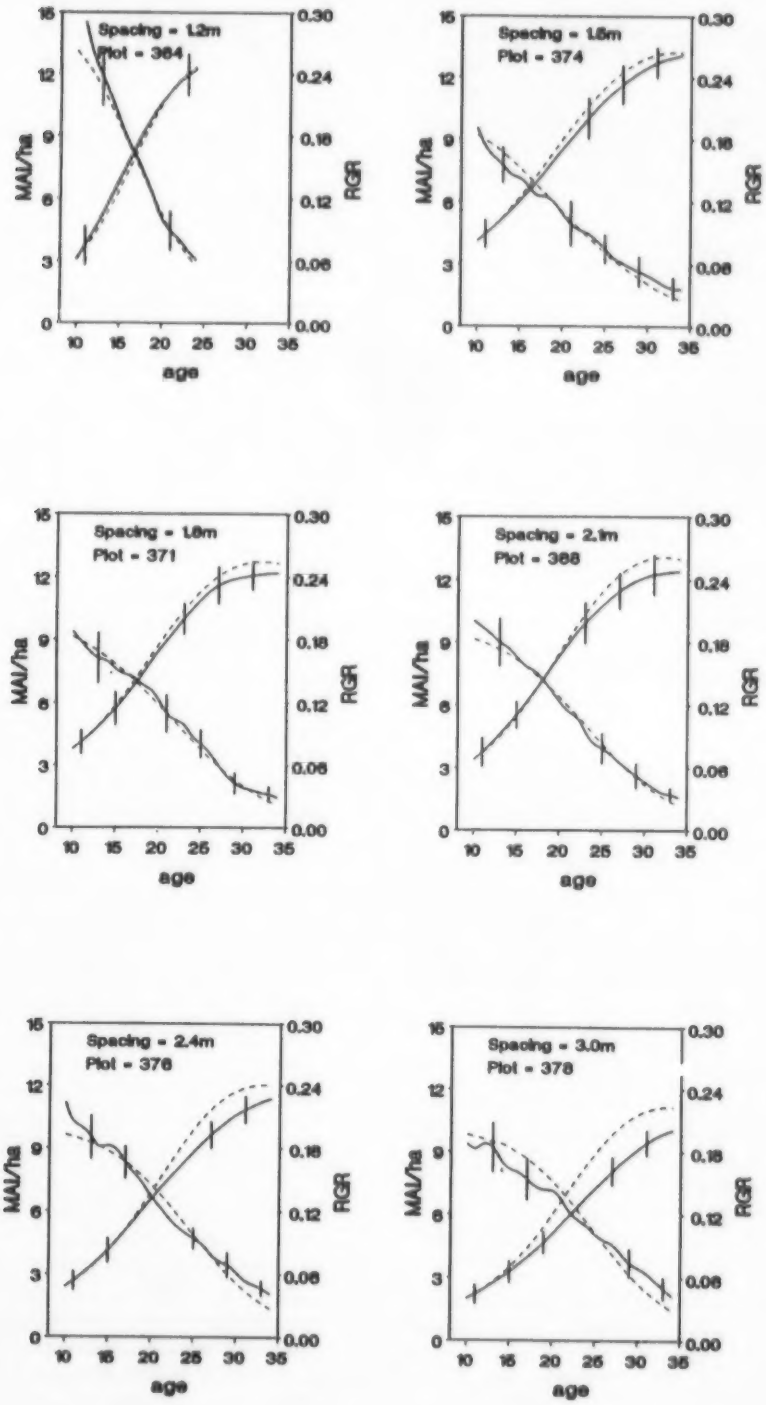

Figure 9. Individual plot model predictions (full line) and observed values (dashed line) of mean RGR (curves descending from left to right) and MAI (curves ascending from left to right). Vertical bars indicate the 68% confidence interval (2x standard deviation of predictions) for the predictions.

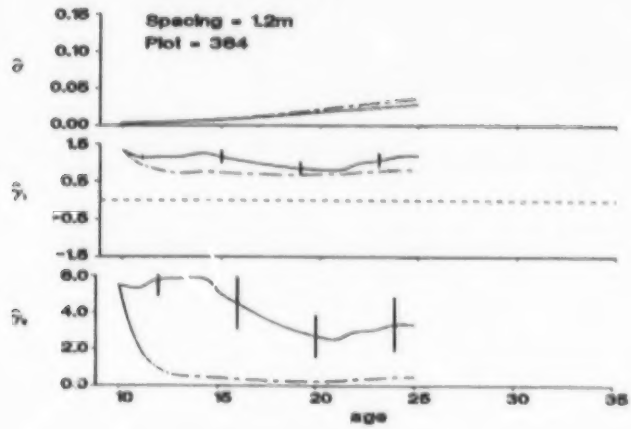

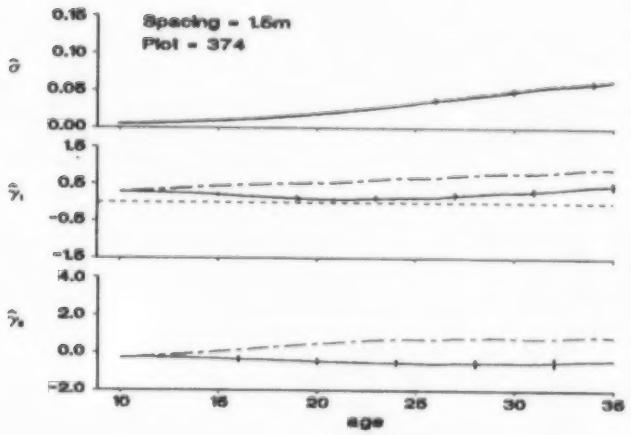

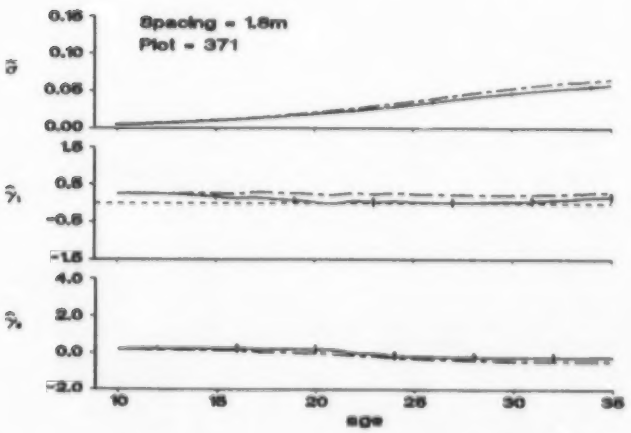

Figure 10. Individual plot model predictions (full line) and observed values (dashed line) of stem volume standard deviation (σ), skewness (γ_1), and kurtosis (γ_2). Vertical bars indicate the 68% confidence interval (2x standard deviation of predictions) for the predictions.

Figure 10 (cont.)

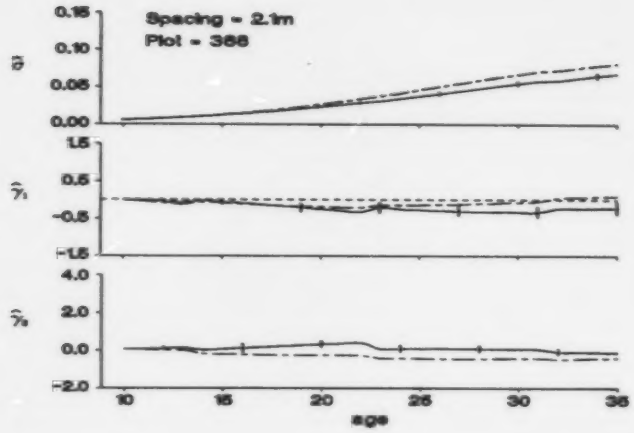

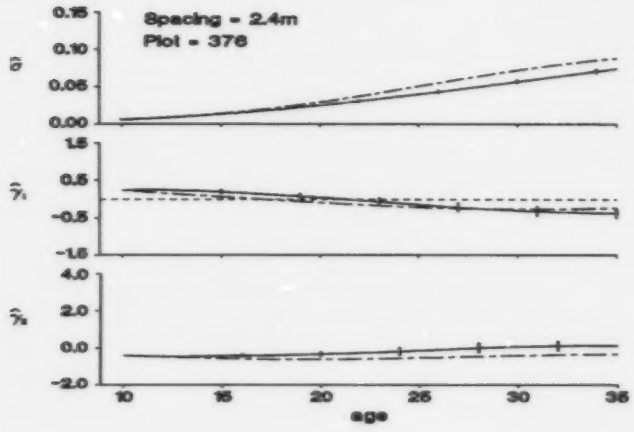

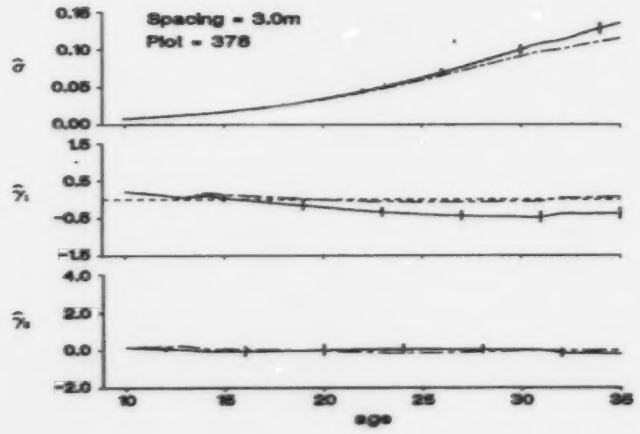

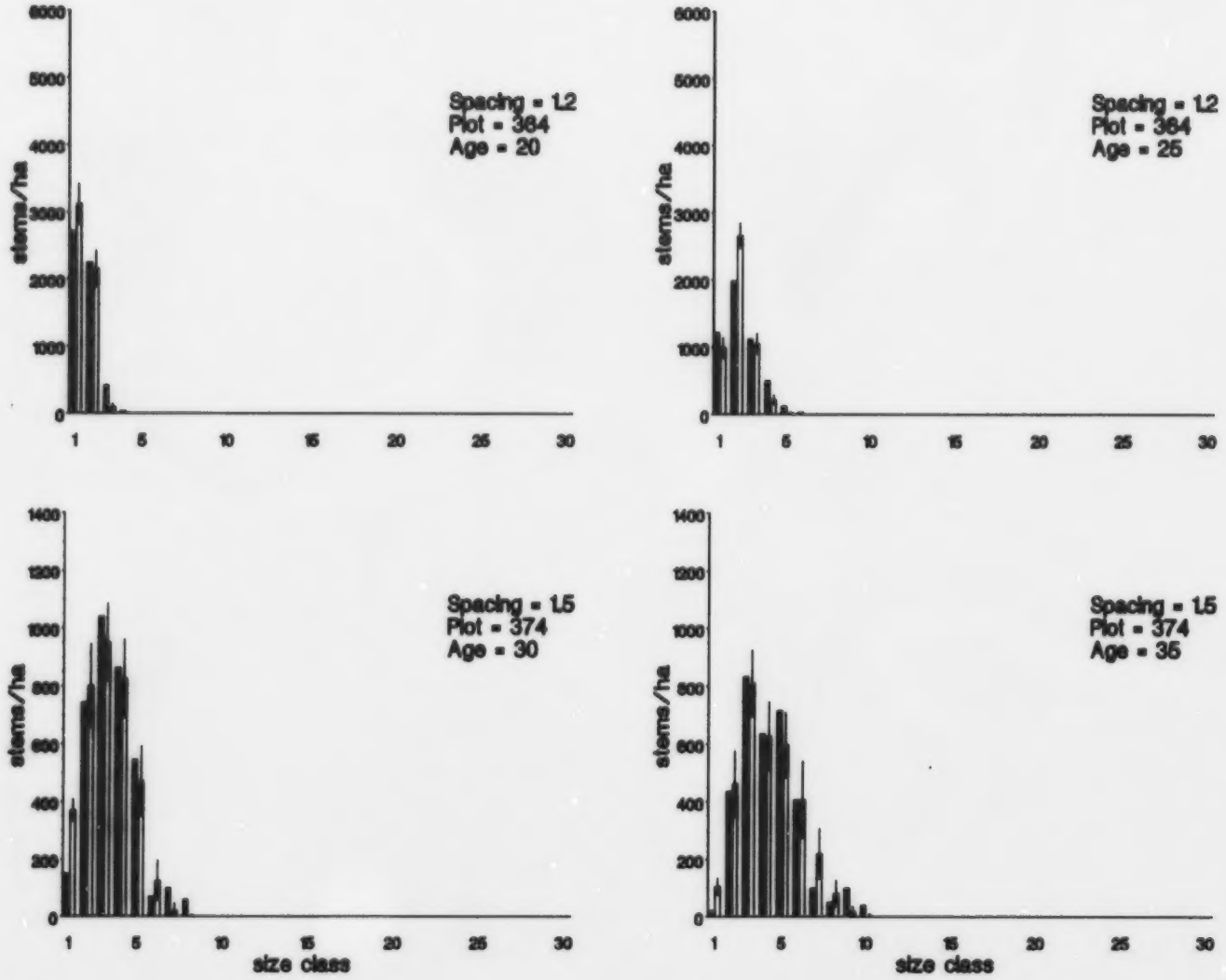

Figure 11. Individual plot model predictions (white bars) and observed values (black bars) of stem size (class width 0.018 m^3) frequencies. Vertical bars indicate the 68% confidence interval (2x standard deviation of predictions) for the predictions.

Figure 11 (cont.)

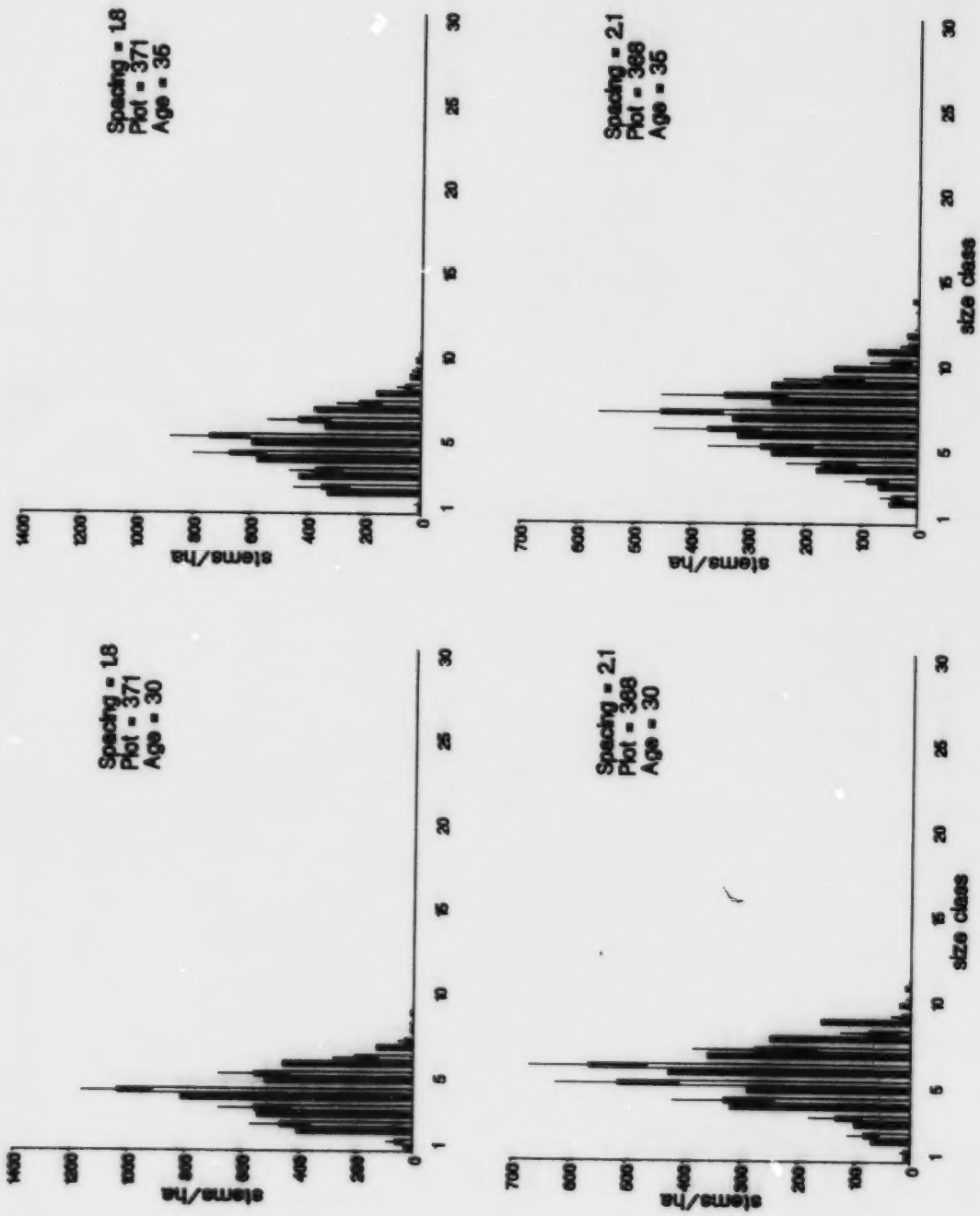

Figure 11 (cont.)

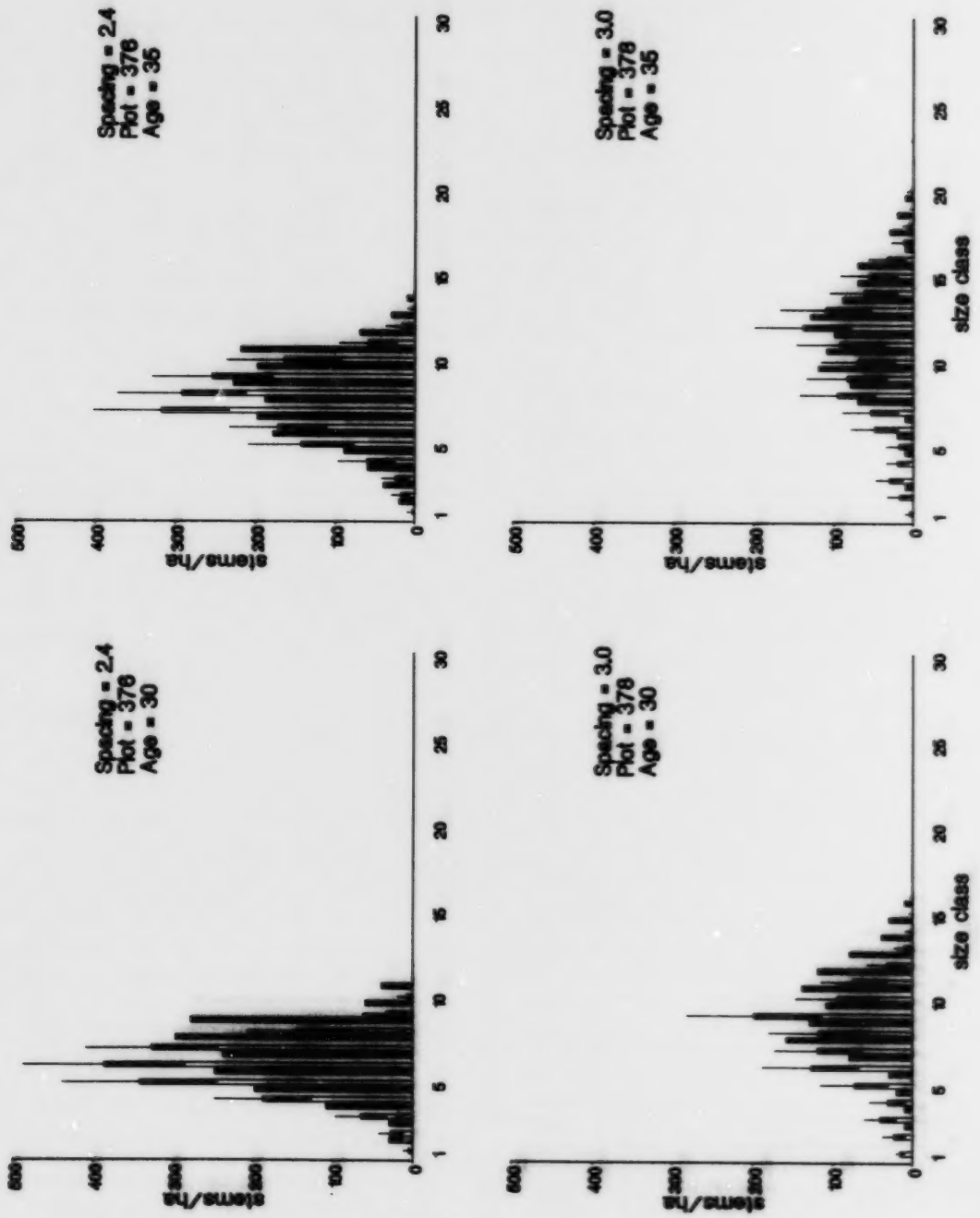

Table 7. Comparisons of individual plot model predictions with 'observed' values of mean volume, maximum volume, relative growth rate, and mean annual increment

Spacing (m)	PSP	Years of predictions	Mean volume		Maximum volume		Relative growth rate (RGR)		Mean annual increment (MAI)	
			Δ%	SEP%	Δ%	SEP%	Δ%	SEP%	Δ%	SEP%
1.2	364	5	3	7	38*[2]	11	3	11	-4	7
		10	-1	8	26*	13	-4	17	-3	6
		15	-1	5	28*	12	35	24	-2	5
	Avg. per year (r)		-0.5[1] (0.94)	-	-1.5 (0.91)	-	1.6 (0.57)	1.3 (0.98)	0.4 (0.75)	0.3 (0.86)
1.5	374	5	-5	5	1	7	-6	12	-8	5
		10	-8	6	-5	8	-2	22	-11	6
		15	-8	7	-12	9	5	19	-9	8
		20	-5	7	-8	9	19	26	-6	8
		25	0	6	-4	9	65	27	-2	6
	Avg. per year (r)		-	-	-	-	1.8 (0.82)	0.7 (0.89)	0.3 (0.79)	-
1.8	371	5	-5	5	-8	7	-3	14	-9*	5
		10	-7	8	-13	9	4	12	-10	9
		15	-6	6	-15	8	7	17	-8	7
		20	-6	4	-11	9	-4	24	-5	5
		25	-4	3	-9	10	54	24	-4	3
	Avg. per year (r)		-	-	-0.3 (0.54)	0.1 (0.83)	-	0.6 (0.91)	-	-
2.1	368	5	-1	6	4	9	1	10	-6	6
		10	-5	6	3	10	-3	15	-7	6
		15	-8	6	-8	8	-5	19	-9	6
		20	-8	5	-14	8	7	29	-8	5
		25	-5	4	-16	7	58*	19	-5	4
	Avg. per year (r)		-0.3 (0.83)	-	-1.0 (0.92)	-	0.8 (0.46)	0.6 (0.72)	-	-
2.4	376	5	-3	6	-1	7	3	11	-7	6
		10	-8	6	-4	6	-8	11	-10	6
		15	-13*	6	-11	6	-4	11	-15	7
		20	-12*	5	-14	6	19	20	-13*	6
		25	-6	4	-13	5	80*	22	-6	4
	Avg. per year (r)		-0.5 (0.74)	-	-0.8 (0.96)	-	1.7 (0.60)	0.6 (0.89)	-	-
3.0	378	5	-9	6	-5	8	-11	14	-12*	7
		10	-19*	7	-12	9	-6	12	-21*	8
		15	-22*	7	-14	8	-1	14	-24*	9
		20	-18*	5	-10	8	26	15	-20*	7
		25	-11*	4	-4	9	76	26	-11*	5
	Avg. per year (r)		-	-	-	-	2.6 (0.82)	-	-	-

Δ% = predicted/observed x 100
SEP% = standard error of predictions in per cent of mean at respective age
r = correlation coefficient between Δ% and years of prediction[1]

[1]Based on all years of predictions.
[2]Level of significance based on t-test (H: observed=predicted), '*' denotes $(P(t>t_\alpha) \leq 0.05$

reflected satisfactorily the already established (see Table 1) effects of initial spacing (see Evert 1971 for references). For example, increasing the initial spacing from 1.5 m to 3.0 m doubled mean stem volume at age 25 and tripled it at age 35. A less pronounced effect was seen in the maximum stem volume; it was approximately 50% larger at a 3.0 m spacing than at 1.5 m spacing. Observed results were similar. Ranks of mean and maximum stem volume by spacing were almost identical ($r_{Spearman} > 0.9$) even after 25 years of predictions.

Comparisons of predictions for individual plots with 'observed' data are visualized in Figures 11 to 15 and quantified in Table 8. It is clear that predictions of the 4.3 m and 6.0 m spacings are subject to considerable errors (bias). These spacings are considered to fall outside the range of practical importance and the results warrant no further analysis.

Predictions of mean stem volume were, on the average, 9% below 'observed' values. An early overestimation of initial relative growth rates (*RGR*) is the most likely explanation for this general model behaviour. The poorest fit was in the 1.2 m spacing and the best fit in the 1.8 m spacing. Relative deviations of predictions from observed values generally reached a maximum after 15 years of predictions beyond which they either stabilized or decreased. On an annual basis, the increase in relative deviations was less than 1.2% per annum. However, when accumulated over time they could exceed 25%. The relative standard error of predictions (SEP%) either increased with the period of prediction or reached a maximum after 10-15 years of predictions. With an average prediction error of approximately 20% none of the deviations were significant at the 5% risk level.

Maximum stem volume predictions were, as a rule, slightly poorer than those of mean stem volume. A tendency of the predictions to drift away from observed values with the length of the prediction period was evident in two plots (365 and 373). Only the 10- and 15-year predictions in the 1.2 m spacing were significantly different from observed values. An annual 1% widening of the gap between observed and predicted maximum values accounted for most of the discrepancies. Note that the prediction of maxima involves only an individual tree. On this basis the model fit is considered satisfactory.

The predicted minimum stem volumes paralleled observed values in all but one plot (366). This result was expected, as mortality was controlled by life tables and not simulated. The discrepancy in plot 366 was caused by the autocorrelation trapping a very small tree into a no-growth mode (there was no mortality in this plot). A simulation of the mortality process would most certainly have eliminated this tree.

Relative growth rates (*RGR*) declined with age in all plots, but more rapidly in the closely spaced plots than in the widely spaced plots (Figure 13). With relative growth rate as the 'engine' in the growth model a good fit to the observations is essential for overall model performance. Although the number of negative deviations equalled the number of positive deviations the latter were, on average, 0.03 too high in the six plots representing the 1.2 m - 3.0 m spacings. The overestimation was serious in the first few years of prediction in plots 365, 373, and 372. Given the compounding effects that even small errors in relative growth rate can have on future volume growth and, in turn, future estimates of *RGR*, it is obvious that an average relative prediction error of 15% (excluding two extreme large relative errors) can lead to the volume bias described above. Our ability to predict the average *RGR* was only moderately successful, as would be expected from the model derivation results (see Table 4 and Figures 6 and 7).

Mean annual increment (MAI) peaked between ages 33 and 35 in the 1.5 m - 2.4 m spacings. An earlier maximum around ages 25 to 27 is indicated in the data from the 1.2 m spacing. Harvest at these ages would secure a maximum sustainable total stem volume production of 12-14 m^3 per hectare per year. The two most widely spaced plots (369 and 385) had reached a MAI of only 7 and 3, respectively, by the last measurement at age 35, with no sign of decline. Predictions of MAI followed in principle the patterns described for RGR and mean stem volume. Fairly accurate predictions (deviations less than 20%) were obtained for the 1.5 m - 2.4 m spacings where discrepancies between predictions and observed values either increased by approximately 0.5% per year (two plots) or remained more or less constant over time (two plots). Predictions for the 1.2 m spacing were off by 17% - 25% with an average bias of 1.2% per year. In the 3.0 m spacing the prediction problem was found to be in the medium term forecasting (10 to 20 years). Standard errors of prediction

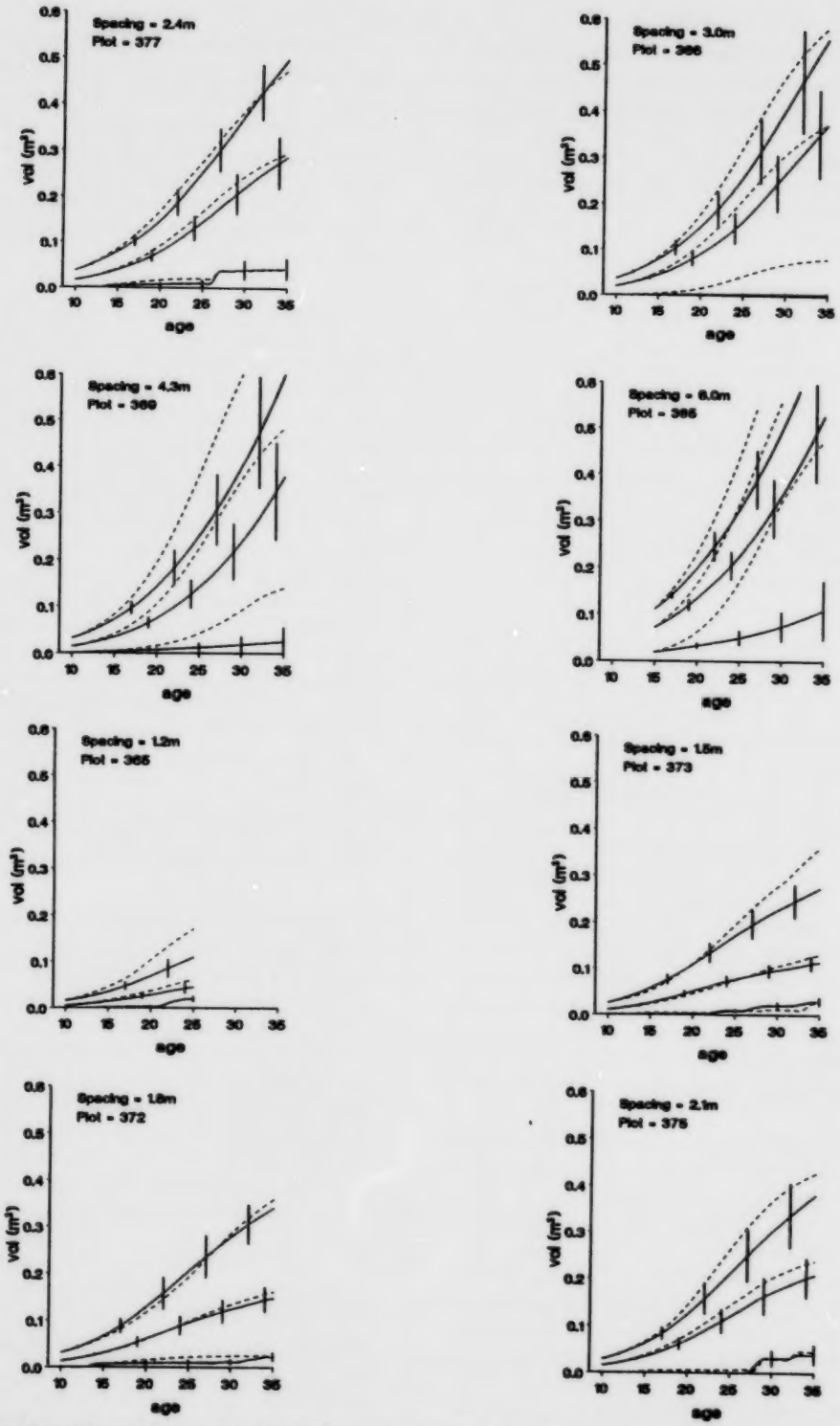

Figure 12. General model predictions (full line) and observed values (dash line) of mean, maximum, and minimum stem volume. Vertical bars indicate the 68% confidence interval (2x standard deviation of predictions) for the predictions.

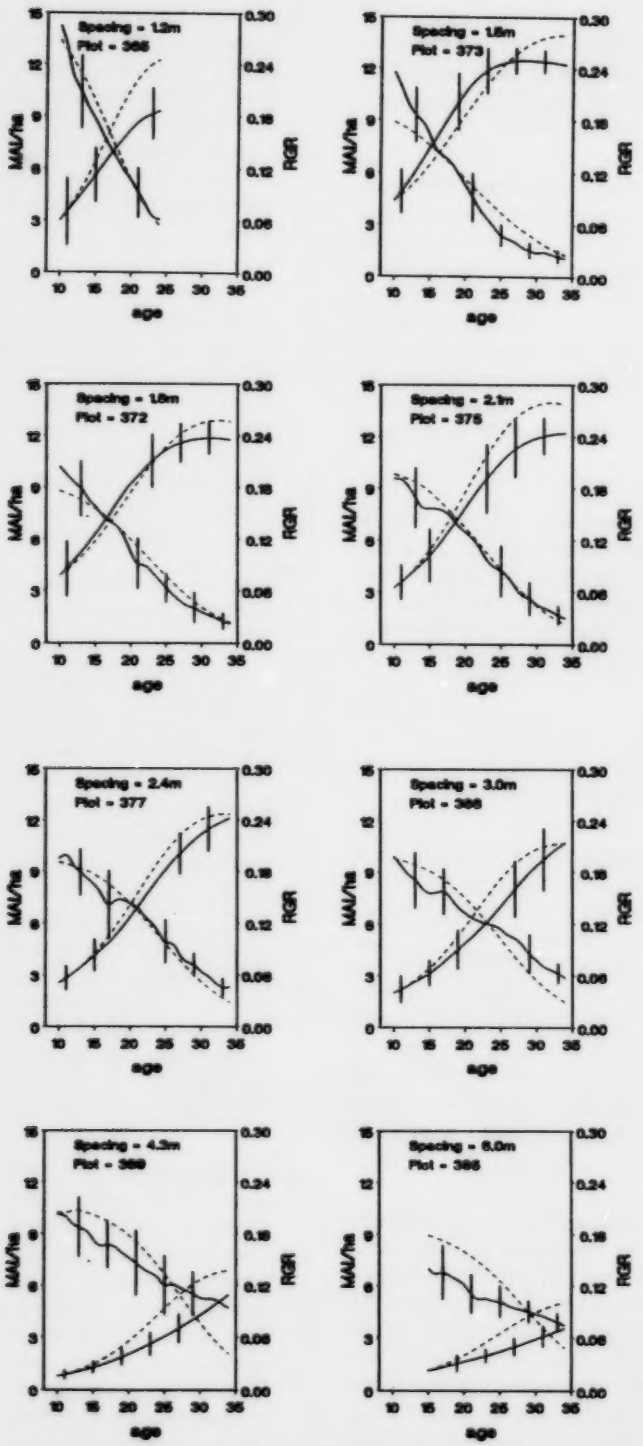

Figure 13. General model predictions (full line) and observed values (dash line) of mean **RGR** (curves descending from left to right) and **MAI** (curves ascending from left to right). Vertical bars indicate the **68%** confidence interval (2x standard deviation of predictions) for the predictions.

(SEP%) averaged about 20%, with a tendency to increase in two plots (365, 366) with length of prediction period. None of the MAI departures were significant at the 5% risk level.

Standard deviations (σ) of observed and predicted plot stem volumes first increased exponentially until an age of approximately 25 years, and then increased at a diminishing rate. There was a good agreement between predicted and observed standard deviations, with one exception. Plot 365 with the 1.2 m spacing was the only example of poor predictions. Predictions for this plot fell increasingly below observed values with time (significant deviations after 10 years of prediction).

Skewness in the frequency distribution of stem volume sizes was positive and statistically significant in the 1.2 m-spaced plot at all ages, and it was significantly negative in the 2.4 m-spaced plot from age 23 and beyond. Skewness (both predicted and observed) remained more or less constant over time. Only in plot 377 did we observe a sudden change from a skewness slightly above zero to a negative value of approx. -0.5. No significant differences emerged between observed and predicted values in any plot.

Kurtosis in the frequency distribution of stem volume sizes was at all ages and in all plots significantly less than 3 which is the expected value of a normal distribution (Snedecor and Cochran 1971). This means that the distributions are platykurtic, or more flat-topped, than the normal distribution. In general, predicted kurtosis reflected observed values well. In plots 365 and 366, however, some of the predicted values did differ significantly from the observations. Kurtosis remained close to zero in all plots regardless of age.

Frequency distributions of predicted and observed stem volumes by size classes (class width = 0.018 m^3) at the last and second last measurements are displayed in Figure 15. Apart from the failure to predict acceptable values for the 4.3 m and 6.0 m spacings, and a statistically significant (1% risk level) departure from the observed distribution in plot 366 at age 30, the remaining predictions were consistent with the hypothesis of no difference between the observed and predicted frequency distribution (test: Kolmogoroff-Smirnov, P(obs.=pred.)>0.20). A Runs test revealed that five of the 12 distributions shown had a significant surplus of one-sided errors through segments of the distributions (i.e. too few alternating positive and negative deviations). The five cases were: plot 365 (age 25), plot 372 (age 30), plot 373 (age 35), plot 375 (age 30), and plot 366 (age 30). Note that in no case did the predicted distribution differ significantly from the observed at both ages shown.

Predictions of stem number in a single size class were not precise. Standard errors of over 100% were common at the extremes. Errors of 10 to 30% were common at the central part of the distributions. A multivariate test of the equality of the two types of distributions (predicted and observed) supported the contention of no significant differences. Predicted distributions were, as expected, more regular than the observed, sometimes 'jagged', distributions.

Discussion and conclusions

Stand growth and yield models based on realistic hypotheses about tree responses to environment (Aikman and Watkinson 1980, Hardwick 1987, Perry 1985, Tait 1988) are better suited to predict outcomes of alternative management options than empirical models. We utilized the fact that tree size itself is the best predictor of growth because a tree's competitive history is integrated in its current size (Ford 1975, Mitchell-Olds 1987, Perry 1985). This approach virtually eliminates any direct influence of age on the growth process and reduces its role to a chronological reference point. With new tissues repeatedly laid down over or replacing older tissues, it is hard to fathom the unique effect of age *per se* unless some physiological aging process occurs (Duff and Nolan 1953 and 1958, Hardwick 1987, Hari and Kellomäki 1981).

Our model also reflects the transition from one-sided competition towards a two-sided process as stand density increases (see Brand and Magnussen 1988). Prior to canopy closure trees compete for light and they acquire resources in proportion to some aspect of their size. After crown closure, when leaf area index and stand assimilation have reached a maximum, smaller individuals get proportionally less light, moisture, and nutrients. This reinforces the size inequality among population members (Ford 1975, Gates 1980). Models based on these principles of distribution-modifying functions, constrained within limits of total yield and individual size,

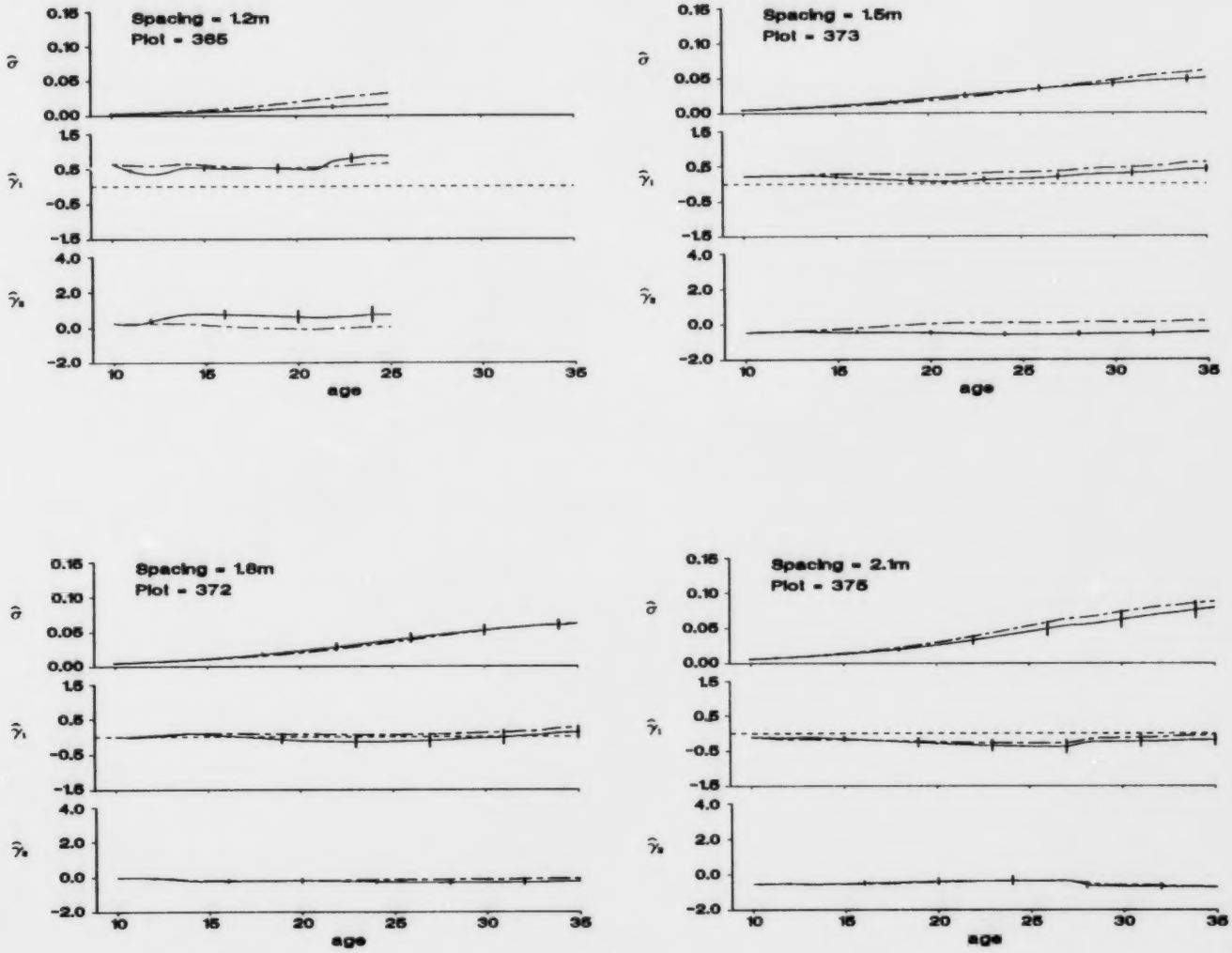

Figure 14. General model predictions (full line) and observed values (dash line) of stem volume standard deviations (σ), skewness (γ_1), and kurtosis (γ_2). Vertical bars indicate the 68% confidence interval (2x standard deviation of predictions) for the predictions.

Figure 14 (cont.)

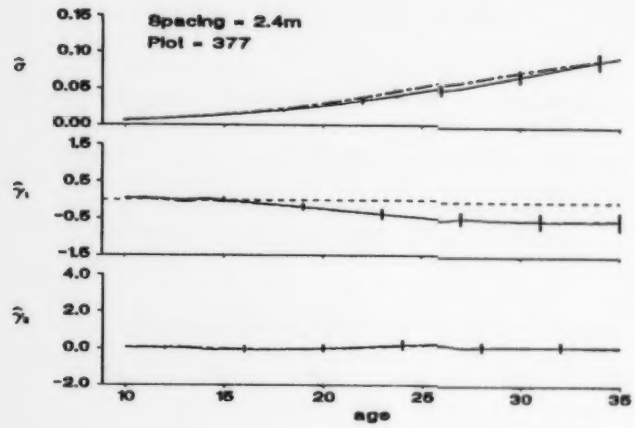

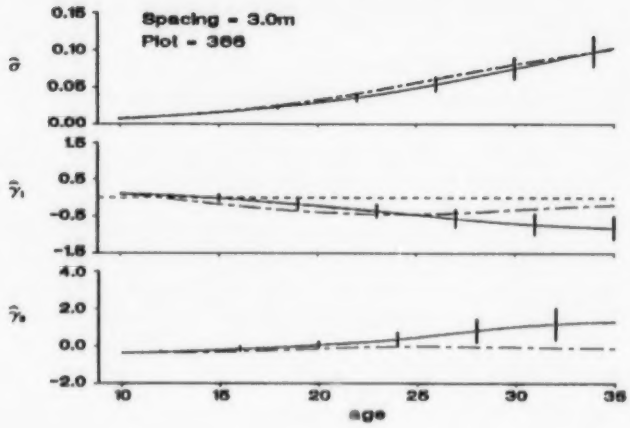

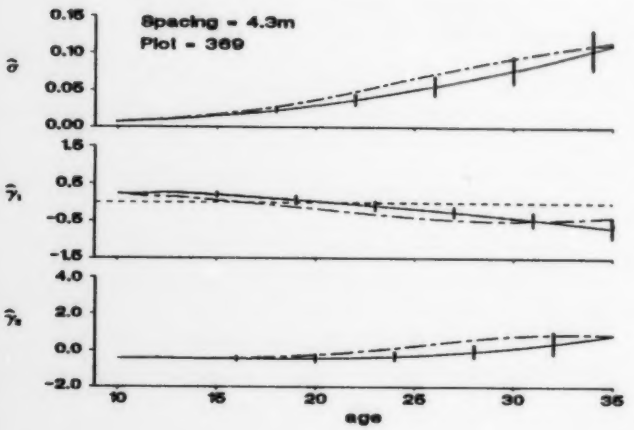

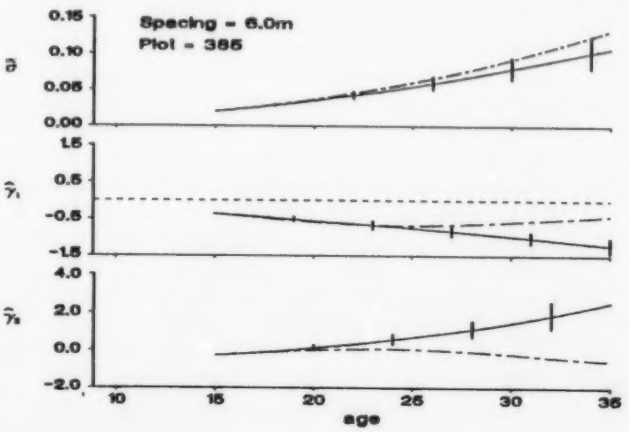

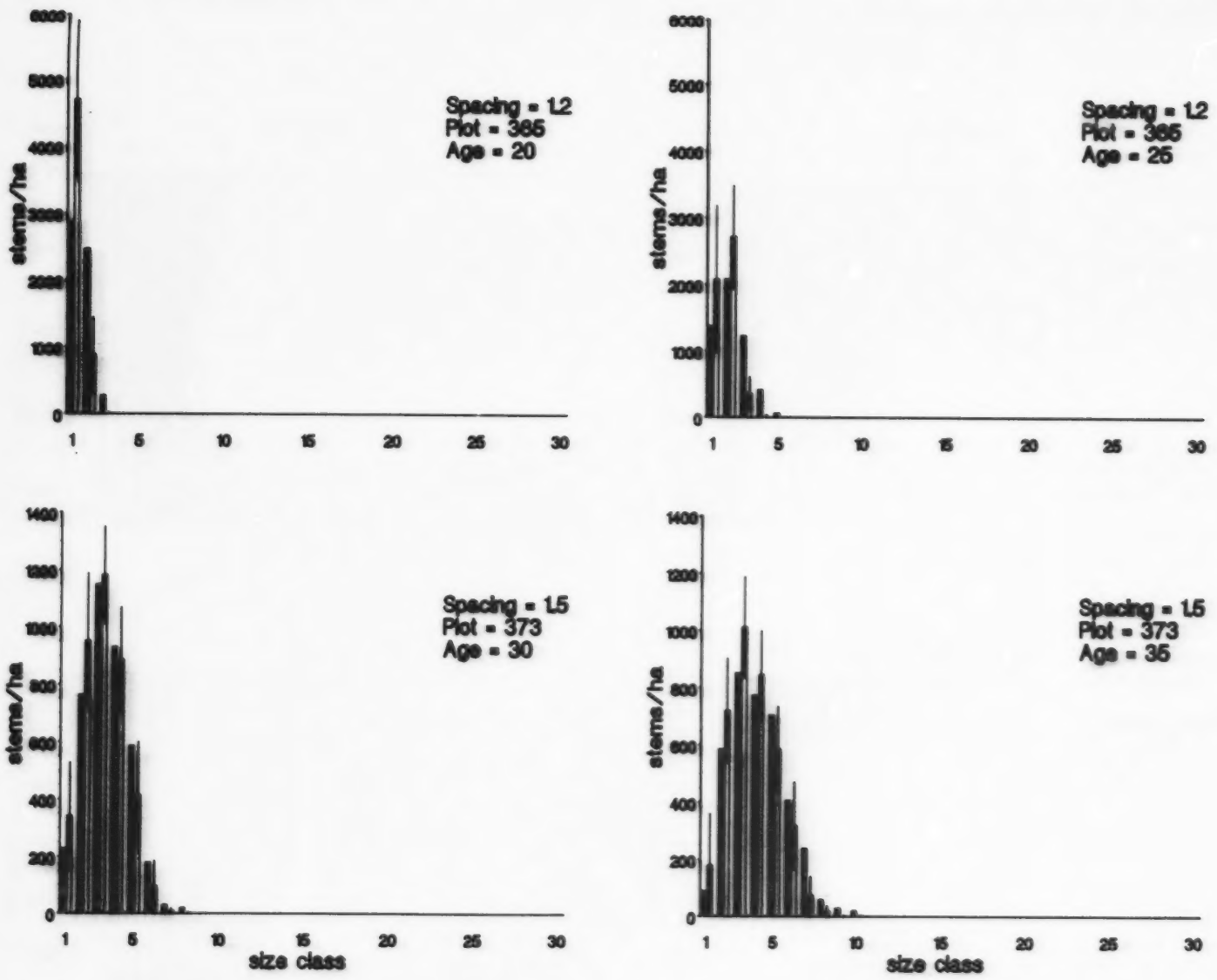

Figure 15. General model predictions (white bars) and observed values (black bars) of stem size (class width 0.018 m^3) frequencies. Vertical bars indicate the 68% confidence interval (2x standard deviation of predictions) for the predictions.

Figure 15 (cont.)

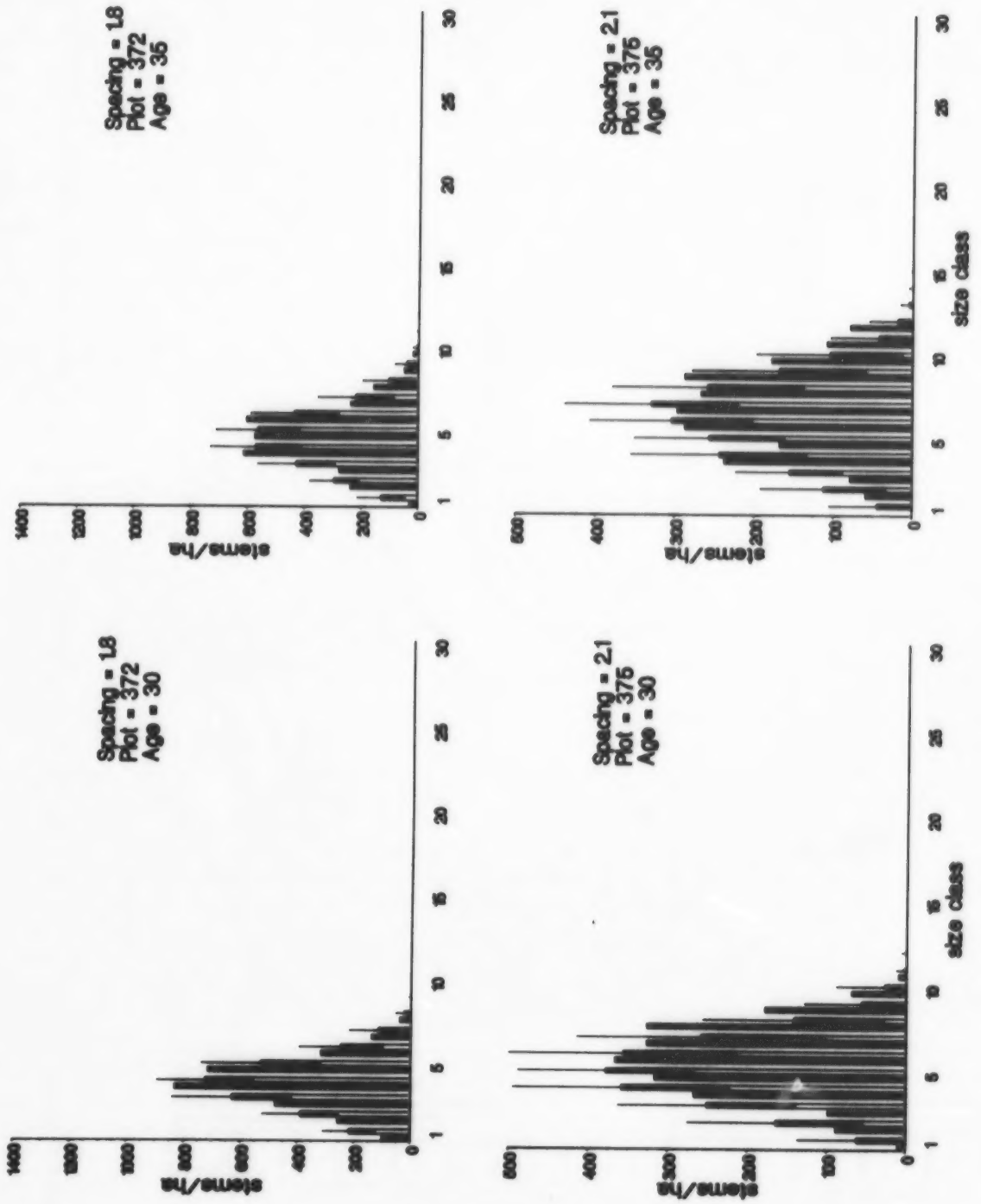

Figure 15 (cont.)

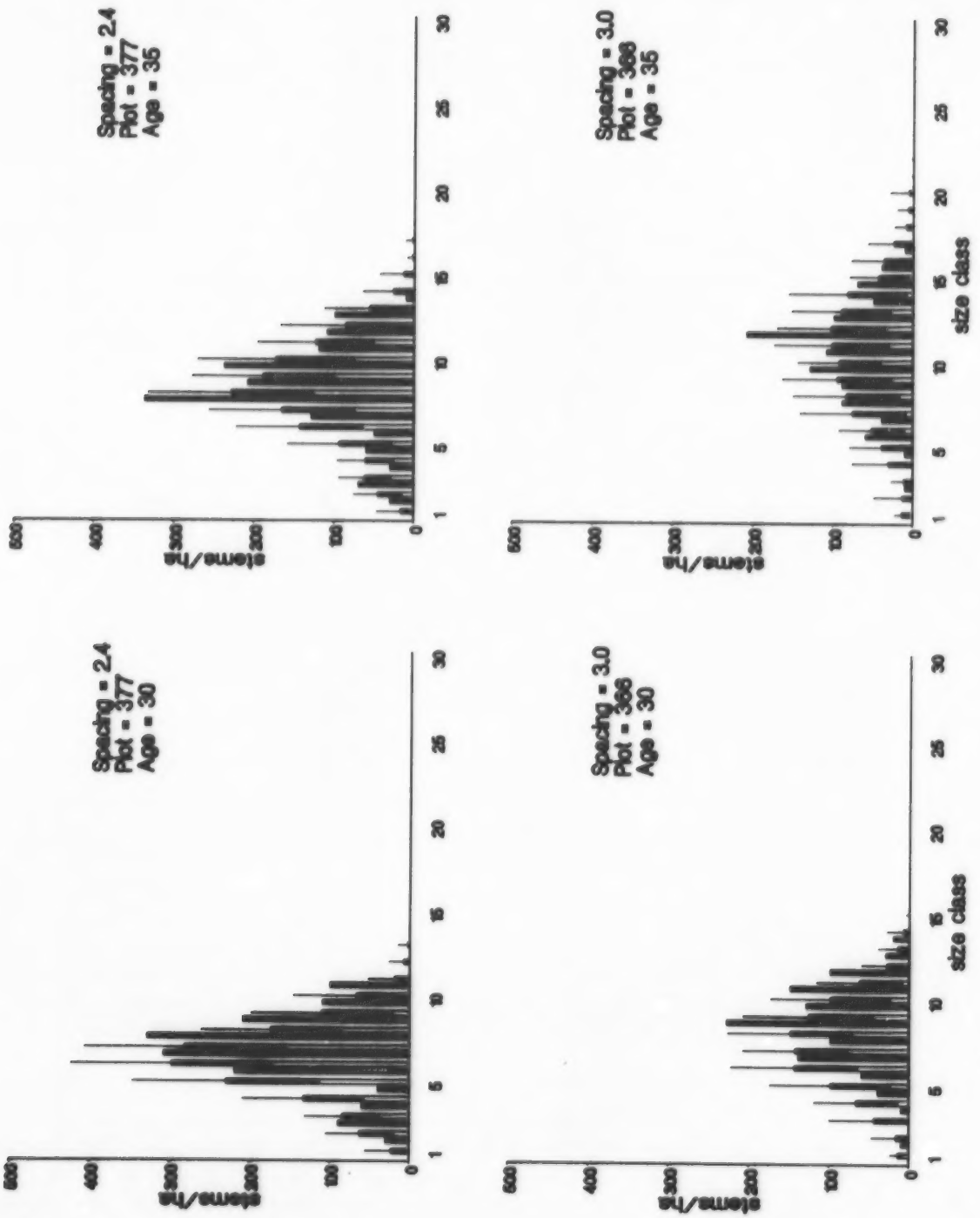

Figure 15 (cont.)

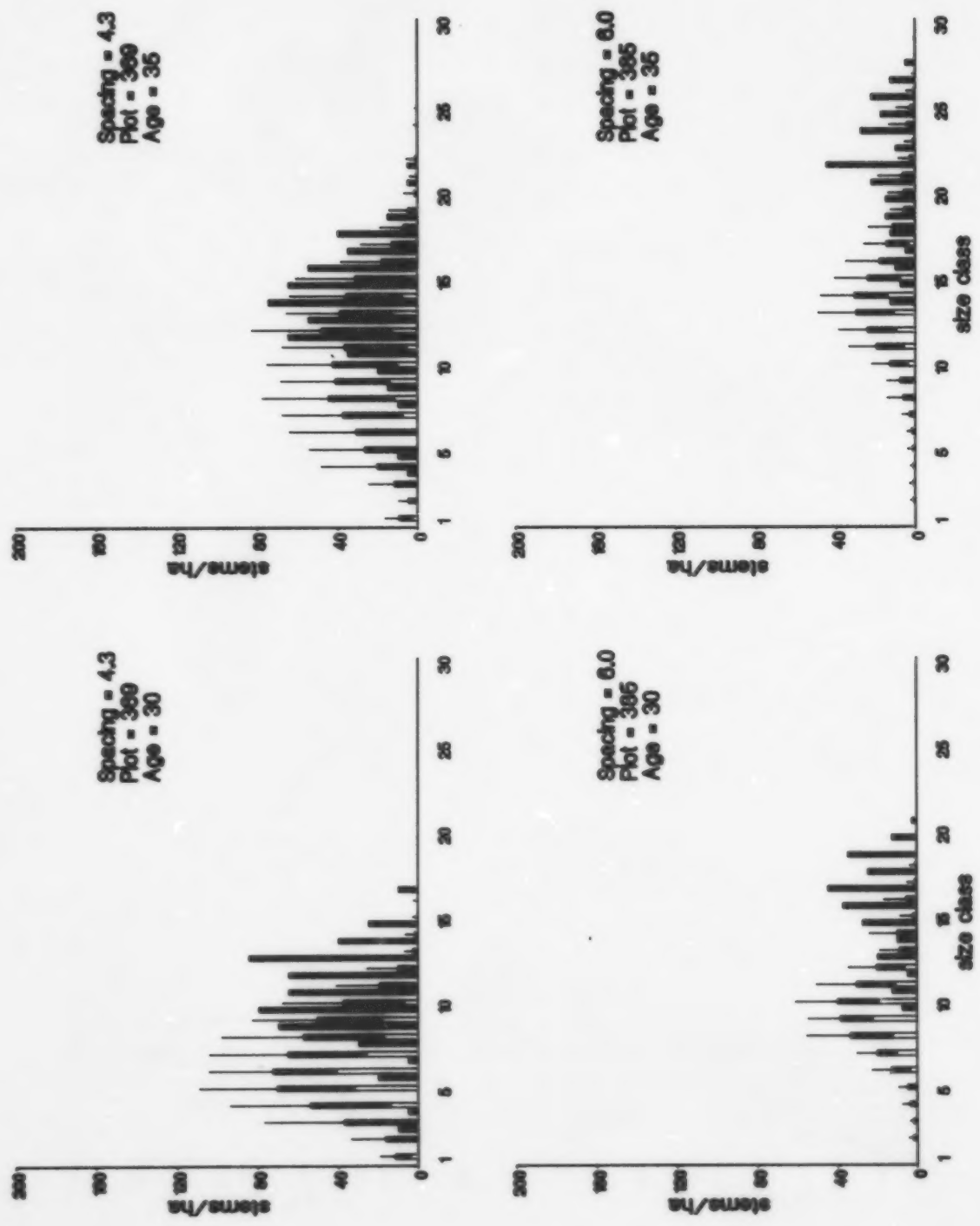

Table 8. Comparisons of general model predictions with observed values of mean volume, maximum volume, relative growth rate, and mean annual increment

Spacing (m)	PSP	Years of predictions	Mean volume		Maximum volume		Relative growth rate (RGR)		Mean annual increment (MAI)	
			Δ%	SEP%	Δ%	SEP%	Δ%	SEP%	Δ%	SEP%
1.2	365	5	-14	13	-22	12	-11	20	-17	15
		10	-24	17	-34*[2]	14	0	37	-25	21
		15	-25	19	-36*	16	40	37	-25	25
	Avg. per year (r)		-1.2[1] (0.92)	1.3	-1.6 (0.96)	1.1	3 (0.82)	2.5 (0.91)	-1.2 (0.87)	2.3 (.094)
1.5	373	5	10	11	11	12	7	19	5	10
		10	12	17	1	15	-2	18	9	16
		15	5	16	-10	13	-29*	26	3	16
		20	-6	14	-17	12	-37*	32	-6	15
		25	-12	12	-23	11	-15	21	-11	14
	Avg. per year (r)		-0.9 (0.79)	-	-1.5 (-0.98)	-	-2.1 (0.78)	-	-0.6 (0.64)	-
1.8	372	5	4	14	6	15	1	17	-1	13
		10	3	21	10	22	-13	32	0	21
		15	3	21	7	22	-17	27	-3	22
		20	-7	18	-2	16	-15	51	-7	19
		25	-8	16	-5	13	10	41	-7	18
	Avg. per year (r)		-0.7 (0.97)	-	-0.7 (0.87)	-	-	1.3 (0.81)	-0.3 (0.70)	0.2
2.1	375	5	-9	12	-5	12	-11	26	-11	13
		10	-14	18	-13	17	-4	22	-16	21
		15	-16	20	-20	18	-2	35	-17	24
		20	-15	20	-18	18	4	43	-15	23
		25	-12	18	-11	17	56	38	-12	21
	Avg. per year (r)		-0.5 (0.77)	0.3 (0.67)	-0.7 (0.77)	-	2.8 (0.83)	0.9 (0.82)	-	-
2.4	377	5	-6	10	-7	9	-7	16	-10	11
		10	-14	15	-13	12	0	15	-17	17
		15	-14	18	-8	14	3	26	-16	21
		20	-10	19	-3	14	23	24	-11	21
		15	-3	20	5	14	93*	23	-4	20
	Avg. per year (r)		-	0.5 (0.94)	0.2 (0.35)	0.2 (0.87)	2.3 (0.76)	0.5 (0.73)	-	-
3.0	366	5	-7	10	-3	11	-13	24	-13	13
		10	-19	17	-15	16	-12	16	-21	20
		15	-22	18	-20	17	11	15	-24	23
		20	-13	22	-15	20	43	23	-16	26
		25	0	27	-4	23	137*	26	-2	27
	Avg. per year (r)		-	0.8 (0.98)	-0.5 (0.50)	0.6 (0.98)	4.4 (0.84)	-	-	0.7 (0.95)

Δ% = predicted/observed x 100-100
SEP% = standard error of predictions in per cent of mean at respective age
r = correlation coefficient between Δ% and year of prediction[1]

[1]Based on all years of predictions.
[2]Level of significance based on t-test (H: observed=predicted), "*" denotes ($P(t>t_2)\leq 0.05$

have been successful in predicting the dynamics of size distributions (Aikman and Watkinson 1980, Benjamin 1988, Ford and Diggle 1981, Gates 1980, Hann and Ritchie 1988, Hara 1984).

A common feature in these models is a growth modifier (like our vigour index 'd') which serves as the link between a potential maximum and observed growth. Through fairly simple relationships to size and stand density, modifiers have proven easier to model than growth itself. Another advantage of the modifiers is the ease of integrating, in a consistent manner, the mortality process in the growth model. Open grown trees are a natural benchmark of potential growth (Assmann 1970, Evert 1971, Ford 1975, Hann and Ritchie 1988, Horne et al. 1986, Perry 1985, Smith and Scott 1984). A size-determined upper limit to growth rate is also implicitly acknowledged in the frequently cited linear relationship between the logarithm of stand density and the logarithm of the average tree size (Hardwick 1987, Sterba 1975, Weller 1987, Yoda et al. 1957, Zeide 1987). As density approaches the occupancy of a single tree, tree size approaches asymptotically towards a constant upper limit. However, our failure to realistically predict growth and yield for the 4.3 and 6 m spacings indicates the need to consider the case where competition is not a driving force in stand development.

Although process-driven growth models furnish no new biological insight *per se* they do provide a means for testing the underlying hypothesized population dynamics (Benjamin 1988, Brand and Magnussen 1988, Gates 1980, Mitchell-Olds 1987). Note, however, that the same data may fit several models equally well (Clutter et al. 1983, Smith and Hann 1986, Sievänen et al. 1988, Tait 1988).

Density effects on stem volume growth are well documented (see Evert 1971 for references) and density management guidelines have been developed for many species (Assmann 1970, Langsaeter 1941, Long 1985, Reineke 1933, Smith and Brand 1987). Our model prepares a suitable framework for simulation of various options of initial spacing. By modelling individual tree growth as a distance independent function of tree size and stand density it circumvents the intricate problems of recovering the size distribution from mean tree and whole stand attributes (Bailey 1980, Hyink and Moser 1979, Martin and Ek 1984). Further, competition effects formulated without spatial information lowers the data requirements for predictions. Spatial independence is based on the assumption that an average diffusion process can adequately describe the competition process (Ford and Diggle 1981, Hara 1984). Spatial analysis of tree size distributions in even-aged plantations have confirmed that the overall negative correlation between the size of neighbouring trees tends to cover considerable microsite variation (Ford 1975, Ghent and Franson 1986, Lorimer 1983, Reed and Burkhart 1985). This type of localized deviation from the average has been recognized in our model through the inclusion of stochastic error terms.

Testing our model on sites different from the experimental location would, of course, inflate prediction errors. Site differences may indeed be the single most significant factor for growth and yield. Further tests of the model on various red pine sites are clearly needed to assess the need for site specific adjustments of maximum growth rates, and of the relationship between *RDI* and the competition coefficients (a and b). Model applications would be severely impeded by a need to recalculate the model for each new site. The costs of doing so are prohibitive. If the need is only for an adjustment of RGR_{max} then the prospects of a wider application appear promising.

Our ability to generate fairly accurate predictions of size-distribution parameters (σ, γ_1, γ_2) indicates a realistic modelling of temporal stand dynamics. The number of size classes displayed in our results far exceeds practical requirements. A reduction to, say, three or four size classes would indicate a much improved fit between observed and predicted distributions.

Relative growth rate is sensitive to competition and, as such, is an obvious candidate for modelling (Aikman and Watkinson 1980, Benjamin 1988, Ford 1981, Ford and Diggle 1981, Hara 1984, Perry 1985). Its major disadvantage rests with the serious compounding effects arising from even minor bias in growth rates. Given the considerable prediction error of a tree's relative growth rate, lasting effects on growth predictions must be anticipated in models relying on RGR. Only the moderating influence of the density index contained predictions within acceptable limits from the observed values.

Errors in forest growth models arises from many sources and their structure can be very com-

plex due to spatial and temporal covariances (Gregoire 1987). Few models provide sufficient information to allow realistic inferences about prediction errors. Most report merely on how well the model fit the data that was used for its derivation. As we have shown, prediction errors arising from stand differences within a given site may be two to three times as high as the errors associated with predictions for a single stand (see also Reynolds et al. 1988). Among-plot variation in growth and yield performance and in sensitivity to competition (see the large among plot variation in predicted *a*- and *b*-values for a given RDI-value) are the main sources of error when results from several plots are pooled to form a single model. Simulation creates an attractive alternative to an analytical approach to error estimation (Ripley 1987). Prediction errors of red pine stem volume growth and yield were often considerable, as expected, but they compared favourably with reported results from other models (Clutter et al. 1983, Ek 1974, Gregoire 1987, Hann and Ritchie 1988, Mitchell 1975, Smith 1983, Smith and Hann 1986, Smith and Scott 1984, Tait 1988).

Some improvement of prediction errors in our model may have been achieved through a simultaneous fitting of related equations (Khuri and Cornell 1987, Reed and Green 1985) instead of using disjointed ordinary least squares (OLS) solutions. Also, an optimized weighting of data with respect to their influence on prediction poses an alternative to our use of simple OLS and arithmetic means. Nevertheless, inferences about errors must await the final judgment of the model users (Reynolds and Chung 1986). Only if the model leads to wrong management decisions, or if yield differs substantially from expectations, do we have an appropriate scale for judging the seriousness of poor predictions. Statistical inferences based on normal theory alone are of little practical use.

References

Aikman, D.P.; Watkinson, A.R. 1980. A model for growth and self-thinning in even-aged monocultures of plants. Ann. Bot. 45:419-427.

Alemdag, I.S. 1978. Evaluation of some competition indices for the prediction of diameter increment in planted white spruce. Can. For. Serv., Inf. Rep. FMR-X-108.

Assmann, E. 1970. The principles of forest yield study: Studies in the organic production, structure, increment and yield of forest stands. Pergamon Press, Oxford.

Avery, T.E.; Burkhart, H.E. 1983. Forest measurements. McGraw-Hill, 3rd ed.

Bailey, R.L. 1980. Individual tree growth derived from diameter distribution models. Forest Sci. 26: 626-632.

Bailey, R.L.; Dell, T.R. 1973. Quantifying diameter distributions with the Weibull function. For. Sci. 19: 97-104.

Belli, K.L.; Ek, A.R. 1988. Growth and survival modeling for planted conifers in the Great Lakes region. For. Sci. 34:458-473.

Benjamin, L.R. 1988. A single equation to quantify the hierarchy in plant size induced by competition within monocultures. Ann. Bot. 62: 199-214.

Borders, B.E.; Bailey, R.L. 1986. A compatible system of growth and yield equations for slash pine fitted with restricted three-stage least squares. For. Sci. 32: 185-201.

Brand, D.G.; Magnussen, S. 1988. Asymmetric, two-sided competition in even-aged monocultures of red pine. Can. J. For. Res. 18: 901-910.

Buchman, R.G. 1985. Performance of a tree survival model on national forests. North. J. Appl. For. 2: 114-116.

Clutter, J.L. 1963. Compatible growth and yield models for loblolly pine. For. Sci. 9: 354-371.

Clutter, J.L.; Fortson, J.C.; Pienaar, L.V.; Brister, G.H.; Bailey, R.L. 1983. Timber management: A quantitative approach. Wiley and Sons, N. Y.

Drew, T.F.; Flewelling, F.W. 1979. Stand density management: an alternative approach and its application to Douglas-fir plantations. For. Sci. 25:518-532.

Duff, G.H.; Nolan, N.J. 1953. Growth and morphogenesis in the Canadian forest species. I. The control of cambial and apical activity in *Pinus resinosa* Ait. Can. J. Bot. 31: 471-513.

Duff, G.H.; Nolan, N.J.. 1958. Growth and morphogenesis in the Canadian forest species. III. The time scale of morphogenesis at the stem apex of *Pinus resinosa* Ait. Can. J. Bot. 36: 687-706.

Ek, A.R. 1974. Nonlinear models for stand table projection in northern hardwood stands. Can. J. For. Res. 4: 23-27.

Evert, F. 1971. Spacing studies - a review. Can. For. Serv., Inf. Rep. FMR-X-37.

Fishman, G.S.; Moore, L.R. 1982. A statistical evaluation of multiplicative congruential random number generators with modulus (2**31)-1. J. Am. Stat. Assn. 7:129-137.

Ford, E.D. 1975. Competition and stand structure in some even aged plant monocultures. J. Ecol. 63: 311-333.

Ford, E.D.; Diggle, P.J. 1981. Competition for light in a plant monoculture modelled as a spatial stochastic process. Ann. Bot. 48: 481-500.

Gates, D.J. 1980. Competition and skewness in plantations. J. Theor. Biol. 94: 909-922.

Gellert, W.; Küstner, H.; Hellwich, M.; Kästner, H. 1975. The VNR Concise Encyclopedia of Mathematics. Van Nostrand Reinhold Co.

Ghent, A.W.; Franson, S.E. 1986. Changes in mortality and size-class spatial distribution patterns in pre-closure and post-closure conifer plantations. For. Sci. 32: 559-575.

Gregoire, T.G. 1987. Generalized error structure for forestry yield models. For. Sci. 33: 423-444.

Hamilton, G.J. 1969. The dependence of volume increment of individual trees on dominance, crown dimension, and competition. Forestry (Oxf.) 42: 133-144.

Hann, D.W.; Ritchie M.W. 1988. Height growth rate of Douglas-fir: A comparison of model forms. For. Sci. 34: 165-175.

Hara, T. 1984. A stochastic model and the moment dynamics of the growth and size distribution in plant populations. J. Theor. Biol. 109: 173-190.

Hardwick, R.C. 1987. The nitrogen content of plants and the self-thinning rule of plant ecology: A test of the core-skin hypothesis. Ann. Bot. 60: 439-446.

Hari, P.; Kellomäki, S. 1981. Modelling of the functioning of a tree in a stand. Stud. For. Suec. 160: 39-42.

Harper, J.L. 1977. Population Biology of Plants. Academic Press.

Harrison, P.J.; Stevens, C.F. 1976. Bayesian forecasting. J. Royal Stat. Soc. Serv. B. 38:205-245.

Holdaway, M.R. 1984. Modeling the effect of competition on tree diameter growth as applied in STEMS. USDA Forest Serv., Gen. Tech. Rep. NC-94.

Horne, R.; Robinson, G.; Gwalter, J. 1986. Response increment: A method to analyze thinning response in even-aged forests. For. Sci. 32: 243-253.

Hunt, R. 1982. Plant growth curves: The functional approach. Edward Arnold, London.

Hyink, D.M.; Moser, J.W. Jr. 1979. Application of diameter distributions for yield projection in uneven-aged forests. Pages 906-916 *in* Frayer, W.E., ed. Forest Resource Inventories. Proc. Wkshp. Vol. II, Colorado State Univ., Fort Collins, July 23-26, 1979.

Hyink, M.; Moser, J.W. Jr. 1983. A generalized framework for projecting forest yield and stand structure using diameter distributions. For. Sci. 29: 85-95.

Kent, B.M.; Dress, P.E. 1980. On the convergence of forest stand spatial patterns over time: the cases of regular and aggregated initial spatial patterns. For. Sci. 26: 10-22.

Khuri, A.I.; Cornell, J.A. 1987. Response surfaces. Design and analyses. Marcel Dekker Inc., New York.

Langsaeter, A. 1941. Thinning in even-aged spruce and pine stands. Medd. Nor. Skogforsoksves. 8: 131-216.

Long, J.N. 1985. A practical approach to density management. For. Chron. 61: 23-27.

Lorimer, C.G. 1983. Tests of age-independent competition indices for individual trees in natural hardwood stands. For. Ecol. Manage. 6: 343-360.

Magnussen, S. 1986. Diameter distributions in *Picea abies* Karst (L.) described by the Weibull model. Scand. J. For. Res. 1: 493-502.

Martin, G.L.; Ek .A.R. 1984. A comparison of competition measures and growth models for predicting plantation red pine diameter and height growth. For. Sci. 30: 731-743.

Mitchell, K.J. 1975. Dynamics and simulated yield of Douglas-fir. For. Sci. Monograph No. 17.

Mitchell-Olds, T. 1987. Analysis of local variation in plant size. Ecology 68: 82-87.

Perry, D. A. 1985. The competition process in forest stands. Pages 481-506 *in* Cannel, M.G.R.; Jackson, J.E., eds. Trees as crop plants. Institute of Terrestial Ecology, NERC, Huntingdon, UK.

Reed, D.D.; Burkhart, H.E. 1985. Spatial autocorrelation of individual tree characteristics in loblolly pine stands. For. Sci. 31:575-587.

Reed, D.D.; Green, E.J. 1985. A method of forcing additivity of biomass tables when using non-linear models. Can. J. For. Res. 15:1184-1187.

Reineke, L.H. 1933. Perfecting a stand density index for even-aged forests. J. Agric. Res. 46:627-638.

Reynolds, M.R. Jr.; Burk, T.E.; Huang, W.-C. 1988. Goodness-of-fit tests and model selection procedures for diameter distribution models. For. Sci. 34: 373-399.

Reynolds, M.R. Jr.; Chung, J. 1986. Regression methodology for estimating model prediction error. Can. J. For. Res. 16: 931-938.

Ripley, B.D. 1987. Stochastic simulation. John Wiley and Sons.

Shifley, S.R.; Brand, G.J. 1984. Chapman-Richards growth function constrained for maximum tree size. For. Sci. 30:1066-1070.

Sievänen, R.; Burk, T.E.; Ek, A.R. 1988. Construction of a stand growth model utilizing photosynthesis and respiration relationships in individual trees. Can. J. For. Res. 18:1207-1035.

Smith, V.G. 1983. Compatible basal area growth and yield models consistent with forest growth theory. For. Sci. 29: 279-288.

Smith, N.J.; Brand, D.G. 1987. Compatible growth models and stand density diagrams. Page 636-643 *in* Ek, A.R. et al., eds. Proc. IUFRO Conf. Forest Growth Modelling and Prediction. Vol. 2. USDA Forest Service, Gen. Tech. Rep. NC-120.

Smith, N.J.; Hann, D.W. 1986. A growth model based on the self--thinning rule. Can. J. For. Res. 16: 330-334.

Smith, F.W.; Scott, D.R. 1984. Derivation of a competitive index for individual trees from seasonal growth patterns. Can. J. For. Res. 14: 266-270.

Snedecor, G.W.; Cochran, W.G. 1971. Statistical methods. 6th ed. Iowa Univ. Press.

Sterba, H. 1975. Assmann's Theorie der Grundflächenhaltung und die "Competition-Density-Rule" der Japaner Kira, Ando und Tadaki. Centralbl. Gesamte Forstwes. 92: 46-62.

Stiell, W.M.; Berry, A.B. 1977. A 20-year trial of red pine planted at seven spacings. Can. For. Serv., Inf. Rep. FMR-X-97.

Tait, D.E. 1988. The dynamics of stand development: a general stand model applied to Douglas-fir. Can. J. For. Res. 18: 696-702.

Weiner, J.; Thomas, S.C. 1986. Size variability and competition in plant monocultures. Oikos 47: 211-222.

Weller, D.E. 1987. Self-thinning exponent correlated with allometric measures of plant geometry. Ecology 68: 813-821.

Westoby, M. 1982. Frequency distributions of plant size during competitive growth of stands: the operation of distribution-modifying functions. Ann. Bot. 50: 733-735.

Wykoff, W.R.; Crookston, N.L.; Stage, A.R. 1982. User's guide to the stand prognosis model. USDA Forest. Serv., Gen. Tech. Rep. INT-133.

Yoda, K.; Kira, T.; Hozumi, K. 1957. Intraspecific competition among higher plants. IX. Further analysis of the competitive interaction between adjacent individuals. J. Inst. Polytechnics, Osaka Univ., Ser. D, Biology. 8:161-178.

Zeide, B. 1987. Analysis of the 3/2 power law of self-thinning. For. Sci. 33: 517-537.